© 2018. Published by The Company of Biologists Ltd | Journal of Cell Science (2018) 131, jcs203828. doi:10.1242/jcs.203828

RESEARCH ARTICLE

SPECIAL ISSUE: PLANT CELL BIOLOGY

Deletion analysis of AGD1 reveals domains crucial for plasma membrane recruitment and function in root hair polarity

Cheol-Min Yoo[1,*], Satoshi Naramoto[2], J. Alan Sparks[1], Bibi Rafeiza Khan[1], Jin Nakashima[1], Hiroo Fukuda[3] and Elison B. Blancaflor[1,‡]

ABSTRACT

AGD1, a plant ACAP-type ADP-ribosylation factor-GTPase activating protein (ARF-GAP), functions in specifying root hair polarity in *Arabidopsis thaliana*. To better understand how AGD1 modulates root hair growth, we generated full-length and domain-deleted AGD1-green fluorescent protein (GFP) constructs, and followed their localization during root hair development. AGD1-GFP localized to the cytoplasm and was recruited to specific regions of the root hair plasma membrane (PM). Distinct PM AGD1-GFP signal was first detected along the site of root hair bulge formation. The construct continued to mark the PM at the root hair apical dome, but only during periods of reduced growth. During rapid tip growth, AGD1-GFP labeled the PM of the lateral flanks and dissipated from the apical-most PM. Deletion analysis and a single domain GFP fusion revealed that the pleckstrin homology (PH) domain is the minimal unit required for recruitment of AGD1 to the PM. Our results indicate that differential recruitment of AGD1 to specific PM domains is an essential component of the membrane trafficking machinery that facilitates root hair developmental phase transitions and responses to changes in the root microenvironment.

KEY WORDS: ADP-ribosylation factor-GTPase activating protein, *Arabidopsis thaliana*, Plasma membrane, Polarity, Root hairs, Tip growth

INTRODUCTION

Root hairs are single-cell projections that emerge from the epidermis of the main root body. These cylindrical cellular projections increase the total surface area of the root, thereby maximizing the uptake of soil resources needed to support the optimal growth and development of the plant (Brown et al., 2012, 2013; Salazar-Henao and Schmidt, 2016). Root hairs expand via tip growth, a process in which membranes and cell wall material are trafficked toward the extreme cell apex (Rounds and Bezanilla, 2013). A wealth of information on mechanisms underlying tip growth control in plants has come from studies on root hair development in the model plant *Arabidopsis thaliana*. For example, detailed microscopic analyses of epidermal cells of post-embryonic *Arabidopsis* roots enabled the identification of discrete growth phases during root hair development. The first phase (phase 1) is characterized by the appearance of a small bulge at the basal (root tip-directed) end of root hair-forming trichoblast cells. This phase is followed by slow expansion of the root hair bulge as it transitions to tip growth (phase 2). In the third phase, tip growth proceeds at a rapid rate leading to the tubular cells typical of root hairs (phase 3) (Dolan et al., 1994). A fourth phase involves the termination of tip growth, characterized by gradual shrinking of the cytoplasm and protrusion of the vacuole to the apical dome (phase 4) (Grierson et al., 2014). The location of root hairs on the root surface has also allowed for convenient forward genetic screens, leading to the isolation of mutants exhibiting a range of root hair polarity defects (Schiefelbein and Somerville, 1990; Parker et al., 2000; Grierson et al., 2001). Detailed studies of these mutants have led to the discovery of a number of proteins that orchestrate tip growth in plants. These include proteins that regulate cytoskeletal dynamics, endoplasmic reticulum morphology, cell wall formation, phosphoinositide (PI) metabolism, lipid modification, monomeric small guanine nucleotide binding protein (small GTPase) cycling, and reactive oxygen species (ROS) signaling (Favery et al., 2001; Seifert et al., 2002; Foreman et al., 2003; Böhme et al., 2004; Carol et al., 2005; Hemsley et al., 2005; Bernal et al., 2008; Thole et al., 2008; Yoo et al., 2008; Lai et al., 2014).

Through a root hair mutant screen in *Arabidopsis*, we identified the ADP-ribosylation factor-GTPase activating protein (ARF-GAP) called AGD1 (ARF-GAP domain 1) (Vernoud et al., 2003) as a regulator of root hair growth directionality, based on the observation that *agd1* mutants exhibited root hairs with wavy/spiral tip growth instead of the straight growth typical of wild-type plants. Furthermore, *agd1* mutants had a large percentage of root hairs with two tips originating from one initiation site, in contrast to the wild type, which had most of its root hairs with only one tip per initiation point (Yoo et al., 2008). Genetic and cell biological studies indicated that AGD1 functions in root hair development through signaling pathways that overlap with those that modulate cytoskeletal remodeling and PI metabolism (Yoo et al., 2012; Yoo and Blancaflor, 2013). However, the precise molecular function of AGD1 in specifying root hair polarity needs further investigation.

ARF-GAPs, the class of proteins to which AGD1 belongs, are best known for their role in regulating cycling of the ARF class of small GTPases. Small GTPases switch between an active and inactive configuration, a process that is essential for their signaling function. When bound to GTP, the small GTPase is active and associates with membranes, where it interacts with a range of effector proteins that mediate cytoskeletal organization and protein trafficking. In yeast, the process of GTP hydrolysis on ARF1 is required for coat disassembly and packaging of cargo during secretory membrane transport (D'Souza-Schorey and Chavrier, 2006). Whereas the switch to the activated, GTP-bound state is facilitated by guanine nucleotide exchange factors (GEFs), GAPs

[1]Noble Research Institute, LLC, 2510 Sam Noble Parkway, Ardmore, OK, 73401, USA. [2]Department of Biomolecular Sciences, Graduate School of Life Sciences, Tohoku University, 2-1-1, Katahira, Aobaku, Japan. [3]Department of Biological Sciences, Graduate School of Science, The University of Tokyo, 7-3-1 Hongo, Bunkyo-ku, Tokyo 113-0033, Japan.
*Present address: Gulf Coast Research and Education Center, University of Florida, 14625 CR 672, Wimauma, FL 33598, USA.

‡Author for correspondence (eblancaflor@noble.org)

S.N., 0000-0002-3373-6343; H.F., 0000-0002-7824-9266; E.B.B., 0000-0001-6115-9670

Received 13 March 2017; Accepted 21 June 2017

Journal of Cell Science (2018) 131, jcs203828. doi:10.1242/jcs.203828

promote hydrolysis of GTP to GDP by converting the small GTPase into its inactive state. Although there is accumulating evidence showing that the GDP-bound forms of small GTPases can have important biological functions, GAPs are generally referred to as small GTPase inactivators (East and Kahn, 2011; Müller and Goody, 2017).

Based on sequence homology, AGD1 is most similar to the ARF-GAP with coiled-coil, ankyrin repeat and PH domain (ACAP) family of mammalian ARF-GAPs. Among the 15 ARF-GAPs in *Arabidopsis*, four are ACAPs or class 1 plant ARF-GAPs (Vernoud et al., 2003). In addition to the GAP catalytic domain, which contains a conserved zinc-binding motif, ACAPs have a Bin1-amphiphysin-Rvs167p/Rvs161p (BAR) and PH domain, and two to three ankyrin (ANK) repeats. The BAR and PH domains function in membrane curvature induction and PI binding, respectively, while the ANK domains enable protein-protein interactions (Vernoud et al., 2003; Gillingham and Munro, 2007; Inoue and Randazzo, 2007). There is accumulating evidence that the additional domains in ACAPs and other multi-domain ARF-GAPs allow them to combine their catalytic GAP activities with other effector scaffolding functions (Donaldson and Jackson, 2011; East and Kahn, 2011). For instance, ACAP2 has been shown to function both as an effector for RAB35 small GTPase and as an inactivator of the ARF6 small GTPase during neurite outgrowth (Kobayashi and Fukuda, 2012, 2013).

In addition to AGD1, another *Arabidopsis* ACAP-type ARF-GAP called AGD3 has been studied using cell biological and genetic approaches. AGD3, also known as VASCULAR NETWORK DEFECTIVE 3 (VAN3) and SCARFACE (SCF), functions in vascular development based on the observation that *agd3* mutants have discontinuous leaf venation patterns (Koizumi et al., 2005; Sieburth et al., 2006). AGD3-GFP fusions were shown to localize to a subpopulation of the trans-Golgi network (TGN)/early endosomes (EE) and the PM, consistent with observations in mammalian ACAPs (Jackson et al., 2000; Koizumi et al., 2005; Naramoto et al., 2009, 2010). The localization of AGD3-GFP is also consistent with the reported endocytic defects of *agd3* mutants (Naramoto et al., 2010). Unlike AGD3, however, the subcellular localization of AGD1 is not known. Such information is important because some *in vitro* studies in mammalian cells have shown that ARF-GAPs have very little differences in ARF substrate specificity. As such, the targeted localization of an ARF-GAP is likely a crucial factor in determining its ARF substrate *in vivo* and, therefore, in explaining a large part of its cellular functions (East and Kahn, 2011).

Here, we used the *Arabidopsis* root hair system to study the localization of a functional AGD1 tagged with GFP to obtain new insight into how an ACAP-type ARF-GAP modulates cell development in plants. We show that AGD1 is recruited to specific PM domains, and that spatiotemporal changes in its localization are correlated with the growth status of root hairs. Based on our results, we propose that differential recruitment of AGD1 to distinct root hair PM domains represents a mechanism to facilitate developmental transitions of root hairs from one phase to another. Furthermore, deletion analysis of AGD1-GFP using an inducible promoter system revealed that the PH domain by binding to specific pools of PIs is the minimal unit that directs AGD1 to the root hair PM, a process that is required for its full functionality.

RESULTS

A functional AGD1-GFP construct is enriched in trichoblasts, and localizes to the PM and cytoplasm

When an AGD1-GFP construct under the control of its native promoter (*AGD1pro:AGD1-GFP*) was expressed in the *agd1* mutant (Yoo et al., 2008), we found that the wavy root hair growth and two root hair tips from one initiation point defects of the mutant were rescued, indicating that the AGD1-GFP construct was functional (Fig. 1A–F). Consistent with the role of AGD1 in root hair development, the AGD1-GFP signal was enriched in root hair-forming trichoblasts (Fig. 1G). Close examination of AGD1-GFP uncovered three patterns of localization in roots. First, AGD1-GFP signal marked the ends of the cells in the primary root meristem and transition zone, a pattern indicative of PM localization. Second, diffuse AGD1-GFP signal within the cell interior also indicated cytoplasmic localization of the construct. Third, AGD1-GFP was associated with punctate bodies of varying sizes (Fig. 1G,H). In root hair cells, some bodies moved slowly while others moved rapidly throughout the cell (Movie 1).

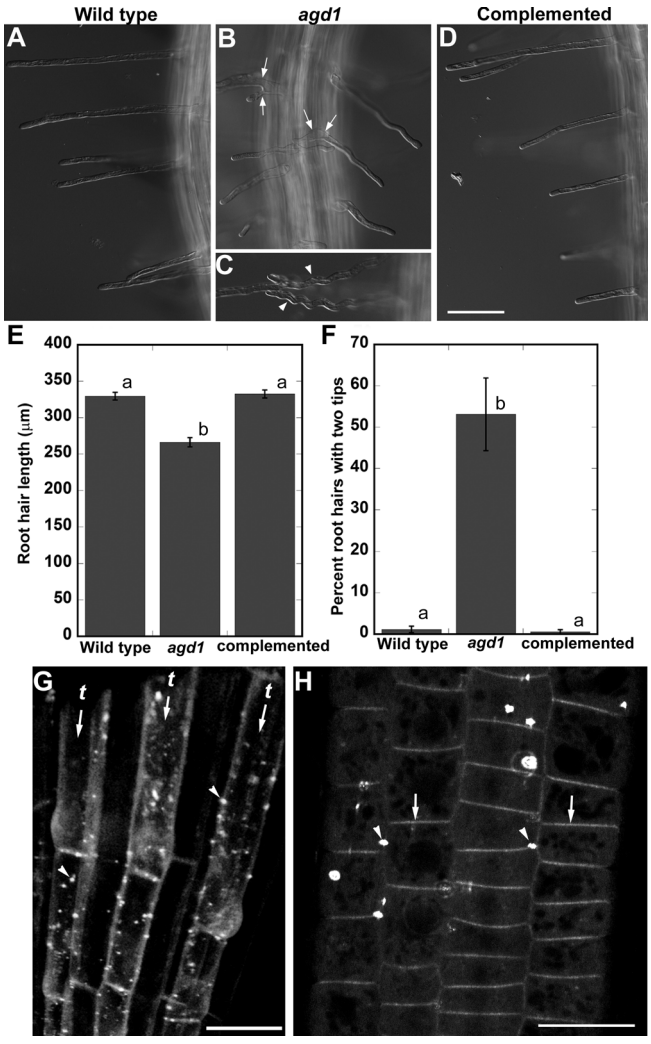

Fig. 1. AGD1-GFP complements *agd1* root hair defects and is enriched in trichoblasts. (A–C) Root hairs of *agd1* mutants have two tips originating from one initiation point (arrows, B) and wavy root hairs (arrowheads, C). (D) Expression of *AGD1pro:AGD1-GFP* complements the *agd1* root hair defects. (E,F) Quantification of root hair length and frequency of root hairs with two tips. Statistical significance was determined by one-way ANOVA. Data are mean±s.e.m. (n=150 root hairs from five independent seedlings). Values marked by different letters are significantly different (P<0.05, Tukey's HSD test). (G) AGD1-GFP signal is most prominent in trichoblasts (*t*, arrows). Cytoplasmic bodies are also labeled (arrowheads). (H) AGD1-GFP in the root meristem and transition zone marks the plasma membrane (arrows) and labels cytoplasmic bodies (arrowheads). Scale bars: 50 µm in A–D; 20 µm in G and H.

Journal of Cell Science (2018) 131, jcs203828. doi:10.1242/jcs.203828

The AGD1-GFP bodies observed in primary roots and root hairs were reminiscent of fluorescent foci typical of the endomembrane system. Furthermore, previous studies of other *Arabidopsis* ARF-GAPs showed that they localized to Golgi and post-Golgi compartments leading us to hypothesize that the AGD1-GFP puncta might also represent known endomembrane organelles (Jensen et al., 2000; Koizumi et al., 2005; Song et al., 2006; Min et al., 2007; Liljegren et al., 2009; Naramoto et al., 2009; Stefano et al., 2010). To test this hypothesis, we generated *Arabidopsis* lines expressing both AGD1-GFP and mCherry markers for the TGN/EE, late endosomes/prevacuolar compartment (LE/PVC) and Golgi (Nelson et al., 2007; Geldner et al., 2009), and asked if the AGD1-GFP bodies colocalized with any of the mCherry endomembrane foci. Surprisingly, confocal imaging of growing root hairs revealed that AGD1-GFP bodies did not overlap with compartments decorated by all of the endomembrane mCherry markers available to us (Fig. 2A–D). Imaging of dual-labeled root cells verified that dynamic green and red bodies corresponding to AGD1-GFP and endomembrane-mCherry fusions, respectively, did not overlap (Movies 2 and 3).

Further verification that AGD1-GFP foci were distinct from post-Golgi compartments was obtained by examining roots treated with Brefeldin A (BFA). Upon exposure to 100 µM BFA, TGN/EE-mCherry markers in the root hair formed fluorescent agglomerates, a behavior typical of post-Golgi organelles (Robinson et al., 2008). However, AGD1-GFP remained in discrete foci that did not overlap with the red-emitting BFA bodies (Fig. 2E). We also treated roots with wortmannin, a chemical that triggers homotypic fusion of the LE/PVC in plant cells. When seedlings were exposed to wortmannin, the PVC markers ARA6 (also known as RABF1)-mCherry and RABF2A-mCherry formed structures that were reminiscent of the fused PVCs reported previously (Wang et al., 2009, 2010). By contrast, AGD1-GFP remained in discrete foci that did not overlap with the red-emitting fused PVC bodies (Fig. 2F).

AGD1-GFP localization to specific PM domains is correlated with root hair growth status

In addition to its localization to unknown foci and the cytoplasm, we found that AGD1-GFP marked the PM of developing root hairs. AGD1-GFP signal in root hair PM was first detected at a domain of the trichoblast where a small root hair bulge formed (Fig. 3A). This observation was in contrast to other proteins known to mark the site of root hair emergence such as the Rho of Plants (ROP) family of small GTPases, which have been reported to accumulate at the PM of the root hair initiation site prior to bulge formation (Molendijk et al., 2001; Jones et al., 2002). Indeed, no AGD1-GFP signal at the PM of root hair initiation sites could be observed in files of trichoblasts in the root transition and elongation zones (Fig. S1A,B). By contrast, in wild-type plants, a ROP2 (also known as ARAC4)-enhanced yellow fluorescent protein fusion (ROP2-EYFP) (Xu and Scheres, 2005) accumulated at the PM of the root hair initiation site prior to the appearance of a root hair bulge (Fig. S1C,D).

We next followed the time course of AGD1-GFP PM localization as root hairs transitioned through the various developmental phases. We found that AGD1-GFP continued to mark the apical-most PM domains of expanding root hair bulges, and as they transitioned to tip growth (Fig. 3B–E; phase 1–2) (Dolan et al., 1994). However, as root hairs proceeded to rapid tip growth (phase 3), AGD1-GFP localization to the apical-most PM domain became less intense and eventually dissipated. Distinct AGD1-GFP signal was confined to the PM of the root hair flanks while gradually weakening as root hairs continued to rapidly elongate (Fig. 3F–H; phase 3). As the

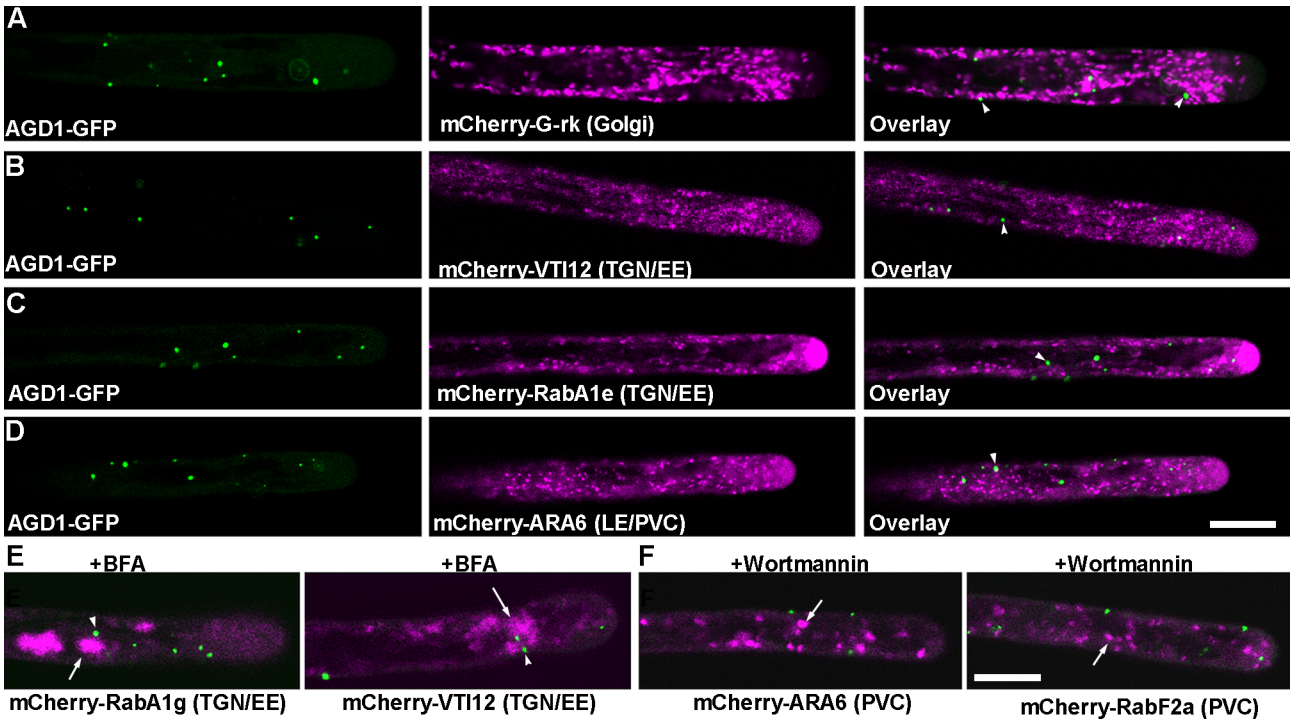

Fig. 2. AGD1-GFP bodies do not colocalize with markers of the endomembrane system. (A–D) Root hair cells expressing AGD1-GFP and mCherry markers to the Golgi, TGN/EE and LE/PVC. The AGD1-GFP bodies (arrowheads) in root hairs at phase 3 do not overlap with mCherry endomembrane foci. (E) mCherry-TGN/EE markers form agglomerates (arrows) when treated with BFA, whereas AGD1-GFP (arrowheads) remains in discrete foci. (F) mCherry-PVC markers form large foci upon treatment with wortmannin (arrows), whereas AGD1-GFP remains in bodies that are distinct from the larger red-emitting fused PVCs. Scale bars: 20 µm.

Journal of Cell Science (2018) 131, jcs203828. doi:10.1242/jcs.203828

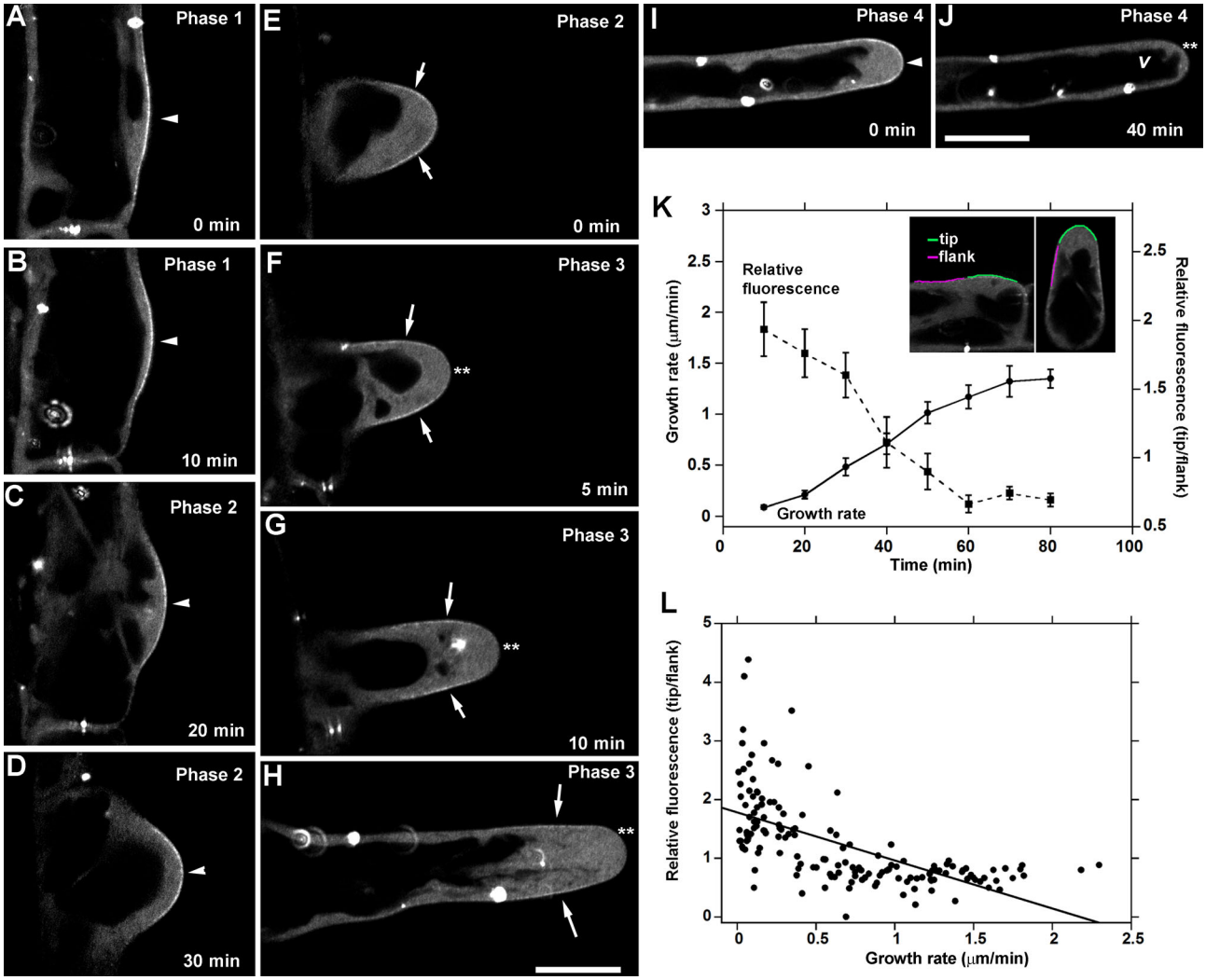

Fig. 3. AGD1-GFP marks specific plasma membrane domains of developing root hairs. (A,B) Distinct AGD1-GFP marks the PM (arrowheads) at the onset of root hair bulge formation. (C,D) As the root hair transitions to tip growth, the AGD1-GFP signal remains at the apical-most PM domain (arrowheads). (E) PM AGD1-GFP signal extends to the lateral PM (arrows). (F–H) During rapid tip growth, PM localization of AGD1-GFP is strongest along the lateral flanks of the root hair (arrows). Weak or no PM labeling is observed at the apical-most PM domain (**). (I–J) As the root hair matures, AGD1-GFP returns to the apical-most PM domain (arrowhead) but then dissipates again as the vacuole (*v*) protrudes closer to the tip (**). (K) PM localization of AGD1-GFP was quantified by obtaining the ratio of relative fluorescence at the apical-most PM domain (green trace in inset) to the shoot-directed PM in bulging root hairs, or root hair flank PM in phase 3 root hairs (magenta trace in inset). Relative fluorescence ratio and growth rate of root hairs at 10 min intervals are presented as a double Y line graph. Data are mean±s.e.m. growth rate and relative fluorescence (n=15 from at least five independent seedlings). (L) A scatter plot reveals a strong inverse relationship between root hair growth rate and relative AGD1-GFP tip/flank fluorescence. Pearson's correlation coefficient=−0.615 ($P \leq 2.2\times10^{-16}$). Scale bars: 20 µm.

root hairs matured and tip growth ceased, intense AGD1-GFP fluorescence returned to the apical-most PM domain (Fig. 3I; phase 4) (Grierson et al., 2014). Finally, AGD1-GFP signal at all PM domains of the root hair dissipated as the cytoplasm dispersed and the vacuole protruded toward the tip (Fig. 3J).

We quantified changes in AGD1-GFP PM localization by obtaining the ratio of PM tip fluorescence to PM fluorescence along the lateral flanks of root hairs. In the case of root hair bulges, PM fluorescence along the more apical (shoot-directed) PM was obtained following the method of Stanislas et al. (2014) (Fig. 3K, inset). Plotting root hair growth rate and the AGD1-GFP tip/flank fluorescence ratio as a function of time in a double Y graph revealed that a higher tip/flank ratio was associated with periods of slower root hair growth (Fig. 3K). Slower root hair growth occurred during the onset of bulge formation and as the root hair transitioned to tip growth (phase 1 and 2) (Dolan et al., 1994), and then again as the root hairs matured (phase 4) (Grierson et al., 2014). During periods of rapid tip growth (phase 3), the tip to flank AGD1-GFP PM fluorescence ratio was significantly lower (Fig. 3K). A scatter plot revealed a strong inverse relationship between root hair growth rate and AGD1-GFP PM fluorescence with a Pearson's correlation coefficient of −0.615 (Fig. 3L). Our results support that AGD1 location at distinct PM domains is correlated with root hair growth status.

AGD1 rapidly relocalizes to the apical-most PM domain when root hair tip growth is prematurely terminated

Whereas AGD1-GFP localization at the apical-most PM domain was associated with slower root hair growth rate during phase 1, 2 and 4, signal at the PM tip dissipated and was confined to the lateral PM in rapidly elongating root hairs at phase 3 (Fig. 3). We therefore hypothesized that when AGD1 is localized to the apical-most PM domain of the root hair tip, it functions in fine-tuning tip growth, most likely as a negative regulator. To test this hypothesis, we

Journal of Cell Science (2018) 131, jcs203828. doi:10.1242/jcs.203828

prematurely terminated the growth of root hairs at phase 3 by subjecting seedlings expressing AGD1-GFP to a hyperosmotic shock using mannitol. Prior to mannitol application, young (~20–30 µm in length) and old (>50 µm in length) root hairs of lines expressing the AGD1-GFP fusion at phase 3 showed the typical flank PM localization and lack of GFP signal at the apical-most PM domain (Fig. 4A). Liquid growth medium supplemented with 500 mM mannitol was then injected into the semi-solid gel that supported the seedling roots, and roots were immediately imaged. Within 1 min of mannitol application, we found intense AGD1-GFP signal at the apical-most PM domain of root hairs at phase 3 that coincided with shrinkage of the tip cytoplasm and stoppage of tip growth (Fig. 4A). We observed that many root hairs at phase 3 were able to resume tip growth within 5–10 min after exposure to mannitol. Resumption of tip growth was accompanied by dissipation of AGD1-GFP fluorescence at the apical-most PM domain and relocalization of the fusion protein to the lateral PM, an observation reminiscent of changes in the localization of the fusion protein as root hairs transitioned from slow tip growth in phase 2 to rapid tip growth in phase 3 (Fig. 4B,C; compare to Fig. 3E–H).

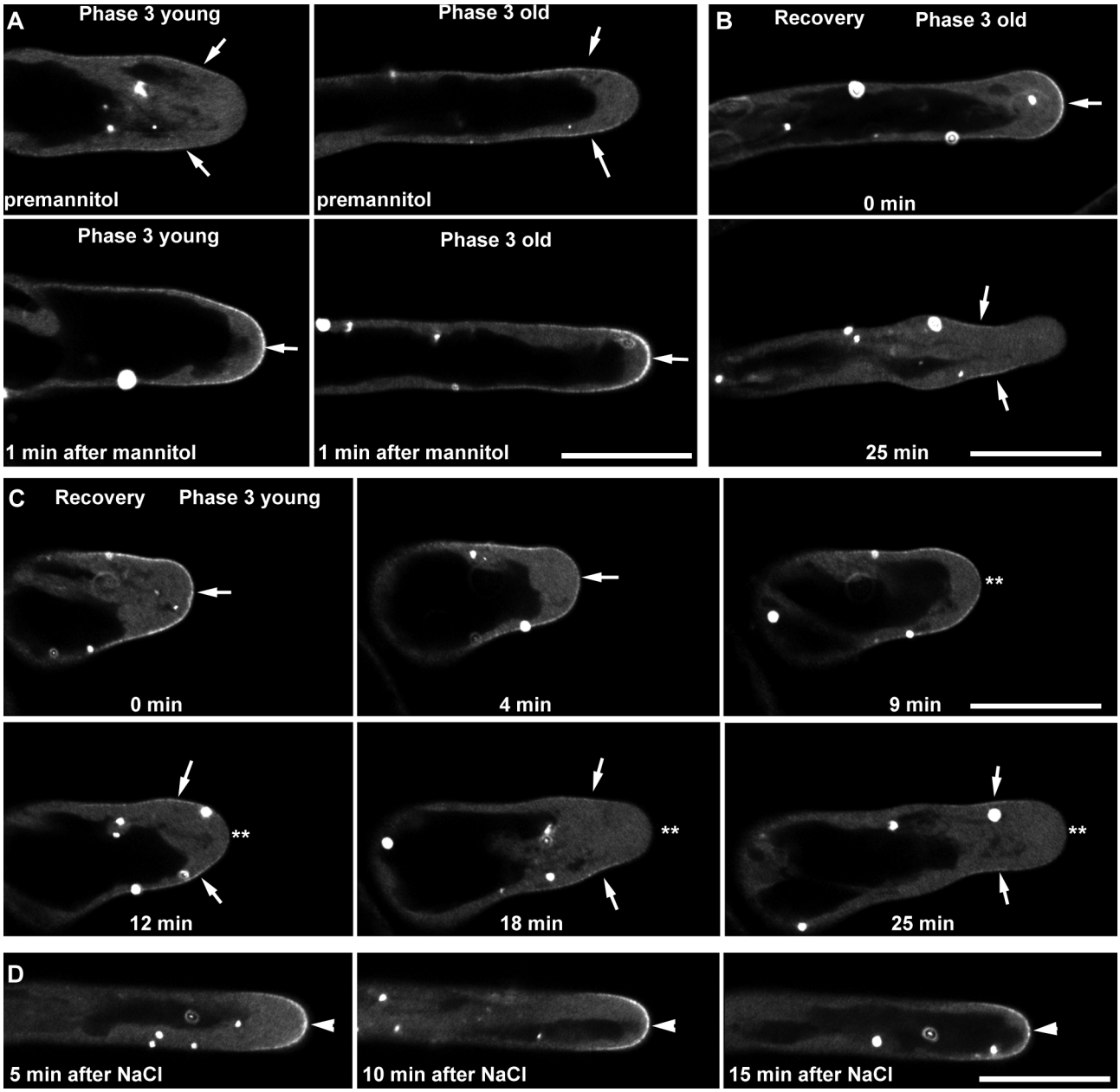

Fig. 4. Premature termination of phase 3 root hair tip growth by hyperosmotic shock leads to rapid relocalization of AGD1-GFP to the apical-most PM domain. (A) Young (<40 µm long) and old (>50 µm long) phase 3 root hairs prior to mannitol treatment show weak AGD1-GFP fluorescence along the lateral PM (diagonal arrows). Within 1 min of mannitol application, intense AGD1-GFP appears at the apical-most PM domain (horizontal arrows). (B,C) Tip growth of root hairs at phase 3 recovers after exposure to mannitol. In old phase 3 root hairs, distinct swelling at the tip is accompanied by intense AGD1-GFP signal (horizontal arrow, B). After 25 min, tip growth has recovered and AGD1-GFP is again confined to the lateral PM (diagonal arrows, B). In a young phase 3 root hair, AGD-GFP at the apical-most PM domain induced by mannitol application (horizontal arrows, C) begins to dissipate after 9 min (**, C). Like old phase 3 root hairs, recovery is associated with AGD1-GFP reverting back to the PM of the lateral root hair flanks (diagonal arrows, C). (D) Phase 3 root hairs treated with 300 mM NaCl are slow to resume tip growth. Distinct AGD1-GFP persists at the apical-most PM domain in these slower growing root hairs (arrowheads). Scale bars: 20 µm.

Journal of Cell Science (2018) 131, jcs203828. doi:10.1242/jcs.203828

The correlation between AGD1-GFP localization to the apical-most root hair PM apex and root hair growth status was also observed in other treatments that inhibited tip growth. For example, like mannitol, treatment with sodium chloride (NaCl) led to relocalization of AGD1-GFP to the apical-most PM domain of phase 3 root hairs within 1 min. However, unlike in mannitol, phase 3 root hairs exposed to NaCl were not able to quickly resume tip growth. As such, localization to the apical-most PM domain persisted in these nongrowing root hairs (Fig. 4D). Taken together, our results support that recruitment of AGD1 to the apical-most PM domain of root hair is associated with root hairs that either grow slowly or terminate tip growth due to an external stimulus.

AGD1 localization to the PM of bulging root hairs is consistent with mild planar polarity defects of *agd1* mutants

Previous characterization of the *agd1* mutant focused on the wavy growth patterns of elongating root hairs at phase 3 (Yoo et al., 2008, 2012). Although the increased frequency of two root hairs emerging from one initiation point in *agd1* mutants is consistent with the localization of AGD1 at the PM of root hair bulges observed here (Fig. 1B and Fig. 3A–C) (Yoo et al., 2008, 2012), it is possible that other phenotypes related to root hair initiation might have been overlooked. We therefore asked whether *agd1* exhibited any planar polarity defects, given that AGD1-GFP localized at the PM during early root hair bulge formation (Fig. 3). In root hair development, planar polarity refers to the position of the root hair initiation site, which is typically directed toward the basal end of the trichoblast (Fischer et al., 2006; Stanislas et al., 2015). We found that there was a slight, but statistically significant, apical (shoot-directed) shift in root hair position in *agd1* mutants compared to wild type (Fig. 5A,B). Like other root hair phenotypes, this mild apical shift in planar polarity was reversed in *agd1* lines expressing the *AGD1pro:AGD1-GFP* construct (Fig. 5B). Our results indicate that AGD1 has a subtle role in defining the position of root hair initiation sites.

The PH domain is required for localization of AGD1 to the root hair PM

The plant class 1 ARF-GAPs are the most complex as they have three other domains in addition to the catalytic GAP domain (Vernoud et al., 2003). However, the contribution of these domains to AGD1 function and subcellular localization has never been addressed. We therefore generated a series of AGD1-GFP constructs with single protein domains deleted. The constructs were placed under the control of an estradiol-inducible promoter (*pER8*) (Zuo et al., 2000) and expressed in the *agd1* mutant background to simultaneously test functionality of the domain deletion constructs and impact of the deleted domains on AGD1 localization. For unknown reasons, we were unable to isolate *agd1* lines expressing AGD1-GFP fusions with only the BAR domain deleted (*pER8:AGD1ΔBAR-GFP*). The constructs we were able to analyze included PH (*pER8:AGD1ΔPH-GFP*), GAP (*pER8:AGD1ΔGAP-GFP*) and ANK (*pER8:AGD1ΔANK-GFP*) domain deletions as well as full-length AGD1 (*pER8:AGD1-GFP*) (Fig. 6A). Non-induced *agd1* mutants expressing *pER8:AGD1-GFP* and all deletion domain constructs showed the root hair polarity defects observed in untransformed *agd1*, including the increased frequency of two root hairs originating from a single initiation point (Fig. 6B; Fig. S2A). By contrast, and consistent with results obtained with the *AGD1pro:AGD1-GFP*-complemented *agd1* lines (see Fig. 1A–F), induction with estradiol rescued the root hair defects of *agd1* expressing the *pER8:AGD1-GFP* construct, indicating functionality of the full-length AGD1 fusion under the

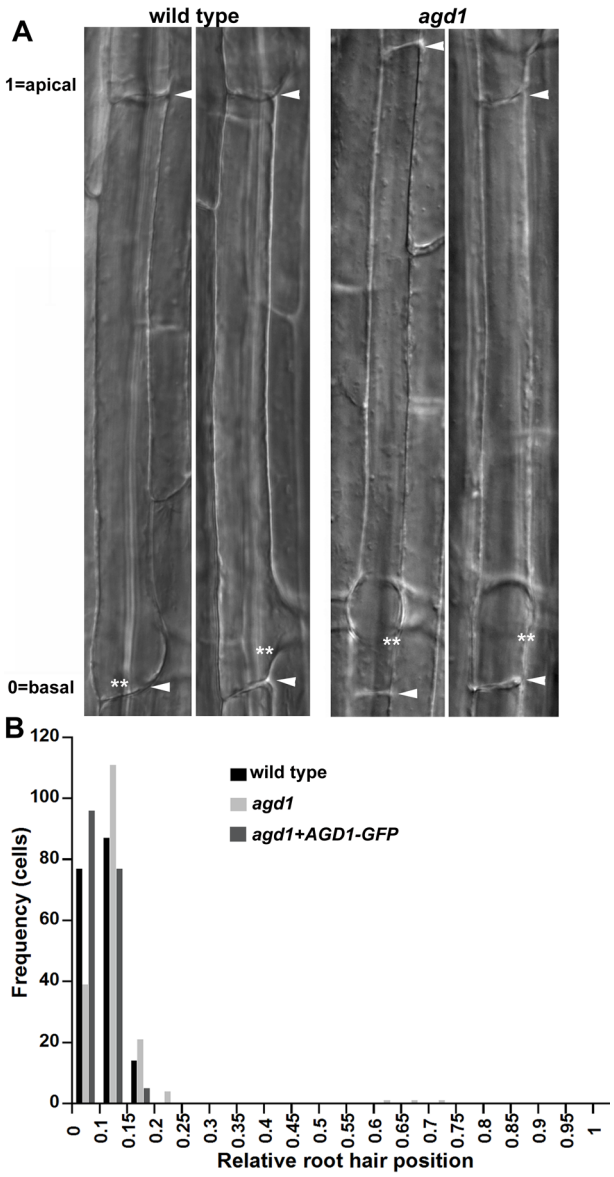

Fig. 5. *agd1* mutants have mild apically shifted root hair planar polarity defects. (A) Differential interference contrast (DIC) microscopy images of two representative trichoblasts from 5-day-old wild-type and *agd1* seedlings. Arrowheads indicate ends of the trichoblast and double asterisks mark the basal wall of the root hair. (B) Quantitative analyses of root hair planar polarity obtained from the images in A. Relative root hair position was obtained by calculating the ratio of the distance from the basal trichoblast wall (bottom arrows in A) to the basal root hair wall (**) over the total length of the trichoblasts. Ratios of relative root hair positions are shown (0=basal; 1=apical). The statistical significance of root hair position distributions among wild type, *agd1* and *agd1* complemented with *AGD1pro::AGD1-GFP* was determined by Kolmogorov–Smirnov test. Wild type versus *agd1* and *agd1* versus *agd1+AGD1-GFP* comparisons were significant ($P<0.01$). The difference in relative root hair position between wild type and *agd1+AGD1-GFP* was not significant ($n=178$ cells were scored for each genotype).

pER8 inducible system (Fig. 6B; Fig. S2B). However, root hair defects of *agd1*-expressing *pER8:AGD1ΔPH-GFP*, *pER8:AGD1ΔANK-GFP* and *pER8:AGD1ΔGAP-GFP* were not rescued by estradiol application (Fig. 6B; Fig. S2C–E).

Upon examination of GFP signals in root hairs of the estradiol-induced seedlings, we found that *pER8:AGD1-GFP* lines showed AGD1-GFP patterns at the root hair PM that mirrored the

spatiotemporal changes observed in the *AGD1pro:AGD1-GFP*-complemented *agd1* lines. Like *AGD1pro:AGD1-GFP* lines, estradiol-induced *pER8:AGD1-GFP* lines showed fluorescent signal that marked the PM of bulging root hairs, the lateral PM of root hairs undergoing rapid tip growth, and the PM at the apical-most PM domain of root hairs that ceased growth (Fig. 6C). AGD1-GFP signal resulting from inducible expression of the *pER8* promoter was generally weaker compared to the *AGD1pro:AGD1-GFP* lines. Furthermore, the unidentified bodies that were typically observed in *AGD1pro:AGD1-GFP*-expressing lines were not as numerous as in estradiol-induced *pER8:AGD1-GFP* lines (Fig. 6C).

We next examined the localization of the three AGD1-GFP domain-deleted constructs after estradiol induction. We found that AGD1ΔPH-GFP no longer marked the PM and was exclusively in the cytoplasm during all phases of root hair development (Fig. 6D). By contrast, AGD1ΔGAP-GFP and AGD1ΔANK-GFP still marked the PM of bulging root hairs and the PM along the flanks of root hairs that proceeded to tip growth, a pattern that roughly mirrored that of full-length AGD1-GFP (Fig. 6E,F). Compared to full-length AGD1-GFP and AGD1ΔGAP-GFP, the signal of AGD1ΔANK-GFP was generally weaker. The AGD1ΔGAP-GFP and AGD1ΔANK-GFP constructs did not complement the *agd1* root hair shape defects, and their localization along the PM flanks of phase 3 root hairs was often asymmetric (Fig. 6E,F). The AGD1ΔPH-GFP and AGD1ΔANK-GFP constructs did not label the unidentified bodies decorated by full-length AGD1-GFP. Although the AGD1ΔGAP-GFP construct also labeled numerous fluorescent aggregates, these foci were smaller and more heterogeneous in size compared to those marked by full-length AGD1-GFP.

AGD1, through its PH domain, is recruited to the root hair PM by binding to enriched pools of PI(4)P

The localization of the AGD1-GFP deletion constructs indicated that the PH domain is required for PM localization. However, because we were unable to isolate plant lines expressing the inducible AGD1ΔBAR-GFP fusion, we could not conclude if the BAR domain contributed to the recruitment of AGD1 to the root hair PM. To address this question, we generated a GFP construct to the AGD1 PH domain alone (*pER8:PH-GFP*) and expressed it in the *agd1* mutant. Upon induction with estradiol, we found that PH-GFP had diffuse signal in the root hair cytoplasm that was more intense than the cytosolic signal observed in full-length AGD1 and the other AGD1-deletion constructs. Despite the strong cytoplasmic signal, PH-GFP could be detected in the PM as the root hair progressed through the different developmental phases (Fig. 7A–F). However, unlike full-length AGD1-GFP or the GAP and ANK AGD1-GFP deletion constructs, PH-GFP was often observed to maintain PM localization at the apical-most PM domain of root hairs (Fig. 7E,F). Like the GAP and ANK deletion constructs, PH-GFP did not complement the *agd1* root hair defects. Localization of PH-GFP was also often observed to be unevenly localized to the PM along the lateral flanks as root hairs developed (e.g. Fig. 7D). PH-GFP tip/flank fluorescence was quantified in a similar manner to that for AGD1-GFP (see Fig. 3K). Like full-length AGD1-GFP, there was an inverse relationship between PH-GFP PM localization and root hair growth rate (Fig. 7G). However, a scatter plot and Pearson's correlation analysis indicated a weaker inverse relationship between PH-GFP PM localization and root hair growth rate (Pearson's correlation coefficient=−0.284) when compared with full-length AGD1-GFP (Fig. 7H).

The PH domain is known to bind PIs. In doing so, proteins that have them are recruited to specific cell membrane regions by binding to PIs that are enriched in that particular membrane (Lemmon et al., 1996). We therefore hypothesized that AGD1, through its PH domain, could be targeted to the root hair PM by binding to specific pools of PIs that are enriched in root hair cells. To test this hypothesis, we first asked whether the AGD1 PH domain alone is capable of directly binding PIs. We cloned the AGD1 PH domain and generated a glutathione-S-transferase (GST)-AGD1-PH domain construct (GST-PH). Purified GST-PH, or GST alone, was used in lipid overlay assays on nitrocellulose strips blotted with a range of phospholipids. We found that GST-PH, but not the GST only controls, bound to PI monophosphates, namely phosphatidylinositol 3-phosphate [PI(3)P], phosphatidylinositol 4-phosphate [PI(4)P] and phosphatidylinositol 5-phosphate [PI(5)P] (Fig. 7I).

Direct binding of the AGD1 PH domain to PI monophosphates prompted us to next ask if the localization of specific PIs in root hair cells mirrored that of PH-GFP. To address this question, we followed the localization of *in vivo* PI(3)P (YFP-2XFYVE) and PI(4)P (YFP-FAPP1) markers (Vermeer et al., 2009) during root hair development. We found that YFP-2XFYVE localized to endosomes and the tonoplast, similar to a previous report (Vermeer et al., 2006), but did not label the PM in phase 1 and phase 2 root hairs (Fig. 7J). By contrast, YFP-FAPP1 marked the PM of root hairs in a similar manner to PH-GFP. Like PH-GFP and full-length AGD1-GFP, YFP-FAPP1 fluorescence was not enriched at the PM of the future root hair initiation site (Fig. 7K). A clear enrichment of YFP-FAPP1 PM fluorescence only became obvious when there was a visible root hair bulge (Fig. 7L). The PI(4)P biosensor continued to mark the PM as the root hair bulge enlarged and proceeded to broadly label the tip and flank PM as the root hairs proceeded to phase 3 (Fig. 7M). As root hairs rapidly elongated, YFP-FAPP1 signal became strongest along the apical 10 µm of the tip, similar to previous reports (Fig. 7N) (Vermeer et al., 2009; Yoo et al., 2012). The enrichment of YFP-FAPP1 along a broad region of the PM apical dome of phase 3 root hairs resembled that of PH-GFP localization (see Fig. 7E,F). Like PH-GFP, YFP-FAPP1 PM localization and root hair growth rate had an inverse relationship (Fig. 7O,P). The similar patterns of PH-GFP and YFP-FAPP1 enrichment during root hair development suggest that enriched pools of PI(4)P recruits AGD1 to the PM. Furthermore, our results on the localization of AGD1ΔPH-GFP (Fig. 6D) and PH-GFP (Fig. 7A-F) support the conclusion that the PH domain is the minimal unit needed for targeting AGD1 to the root hair PM.

DISCUSSION

We used the root hair system of *Arabidopsis* to gain a deeper understanding of the role of an ACAP-type ARF-GAP in specifying plant cell polarity. Plant root hairs are tubular extensions of root epidermal cells that develop through a series of distinct phases (Dolan et al., 1994; Grierson et al., 2014). Like pollen tubes, fungal hyphae and neurons, root hairs expand via tip growth, leading to a cellular geometry with an extreme aspect ratio in which the length of the cell is several times its width. For tip-growing plant cells to maintain this extreme aspect ratio, material for constructing the cell wall has to be transported over long distances and targeted to the apical-most PM of the cell (Chebli et al., 2013). The convenience of the root hair system for live cell microscopic and genetic studies has led to the identification of several key proteins that are part of the tip-growth machinery in plants. In many cases, localization of these proteins to the root hair tips using GFP fusions has validated their importance for root hair development (Kusano et al., 2008; Stenzel et al., 2008; Thole et al., 2008; Park et al., 2011; Park and Nebenführ, 2013). Here, we provide evidence that the ARF-GAP

Journal of Cell Science (2018) 131, jcs203828. doi:10.1242/jcs.203828

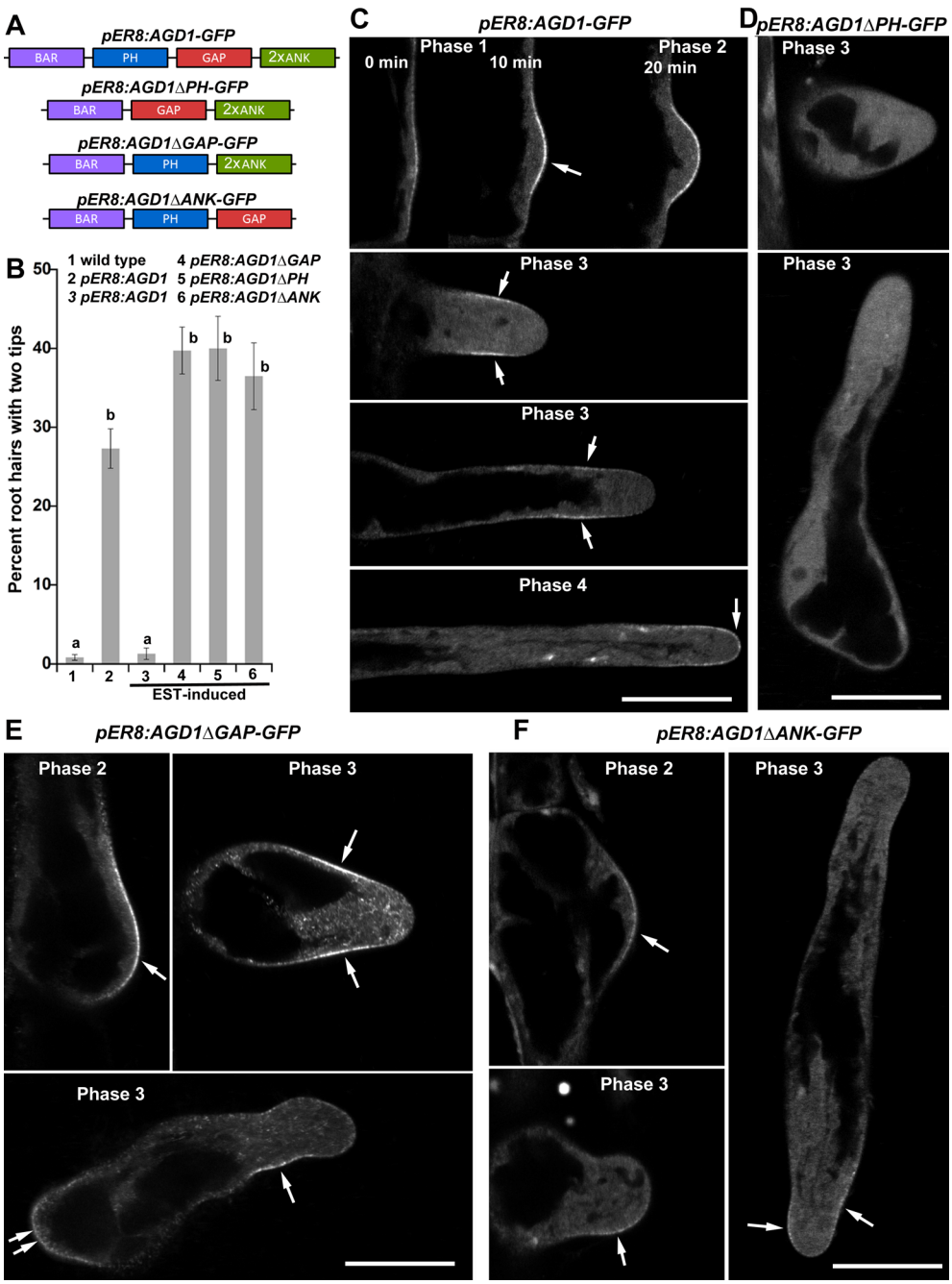

Fig. 6. The PH domain is required for AGD1 localization to the root hair PM. (A) Schematic of inducible full-length AGD1-GFP and domain-deleted constructs. (B) Induction of *agd1* mutants expressing full-length AGD1-GFP, but not the deletion constructs, with estradiol (EST) rescues the two root hair tip phenotype. Statistical significance was determined by one-way ANOVA. Data are mean±s.e.m. (n=257 root hairs from 15 independent seedlings). Values marked by different letters are significantly different (P<0.05, Tukey's HSD test). (C) Localization of full-length AGD1-GFP at the root hair PM (arrows) after estradiol induction. (D) AGD1ΔPH-GFP is located exclusively in the cytoplasm. (E,F) AGD1ΔGAP-GFP and AGD1ΔANK-GFP still mark the PM (arrows) at various phases of root hair development. PM localization of AGD1ΔGAP-GFP and AGD1ΔANK-GFP were asymmetric, particularly in root hairs with irregular shapes and two tips (arrows). Scale bars: 20 µm.

AGD1 is another root hair tip-localized protein. Based on its localization patterns at the root hair apex, we propose that AGD1 is an important component of the secretory apparatus that defines polarized root hair growth through its timely depletion or displacement from, and recruitment to, specific PM domains.

Although several studies have demonstrated tip-directed protein localization in *Arabidopsis* root hairs using fluorescent protein fusions, not many have followed details of their spatiotemporal changes during root hair development, or in response to treatments that suppress tip growth. In studies in which such experiments were conducted, tip-directed functional YFP-cellulose synthase-like 3 (YFP-CSLD3) and YFP-myosin-17 (YFP-XIK) were monitored in root hairs treated with the actin disrupting drug latrunculin B (LatB) (Park et al., 2011; Park and Nebenführ, 2013). A rapid loss in tip-directed YFP-CSLD3 and YFP-XIK localization was observed within minutes of LatB treatment that coincided with a decline in root hair growth (Park et al., 2011; Park and Nebenführ, 2013). In the case of YFP-CSLD3, its accumulation at the tip and resumption of root hair growth was restored upon LatB washout (Park et al., 2011). The spatiotemporal patterns of CSLD3 and XIK localization during root hair development are examples of proteins that positively regulate tip-focused expansion. Their role as positive regulators of tip growth is consistent with *xik* mutants having short root hairs, while those of *csld3* rupture at the tip soon after initiation (Wang et al., 2001; Bernal et al., 2008; Kusano et al., 2008; Stenzel et al., 2008; Park and Nebenführ, 2013). By contrast, our data indicate that AGD1 partly functions to restrict growth since its depletion at the apical-most PM domain coincides with rapid tip growth. Evidence to this effect can be seen by enhanced AGD1-GFP signal at the apical-most PM domain when root hair growth is

Journal of Cell Science (2018) 131, jcs203828. doi:10.1242/jcs.203828

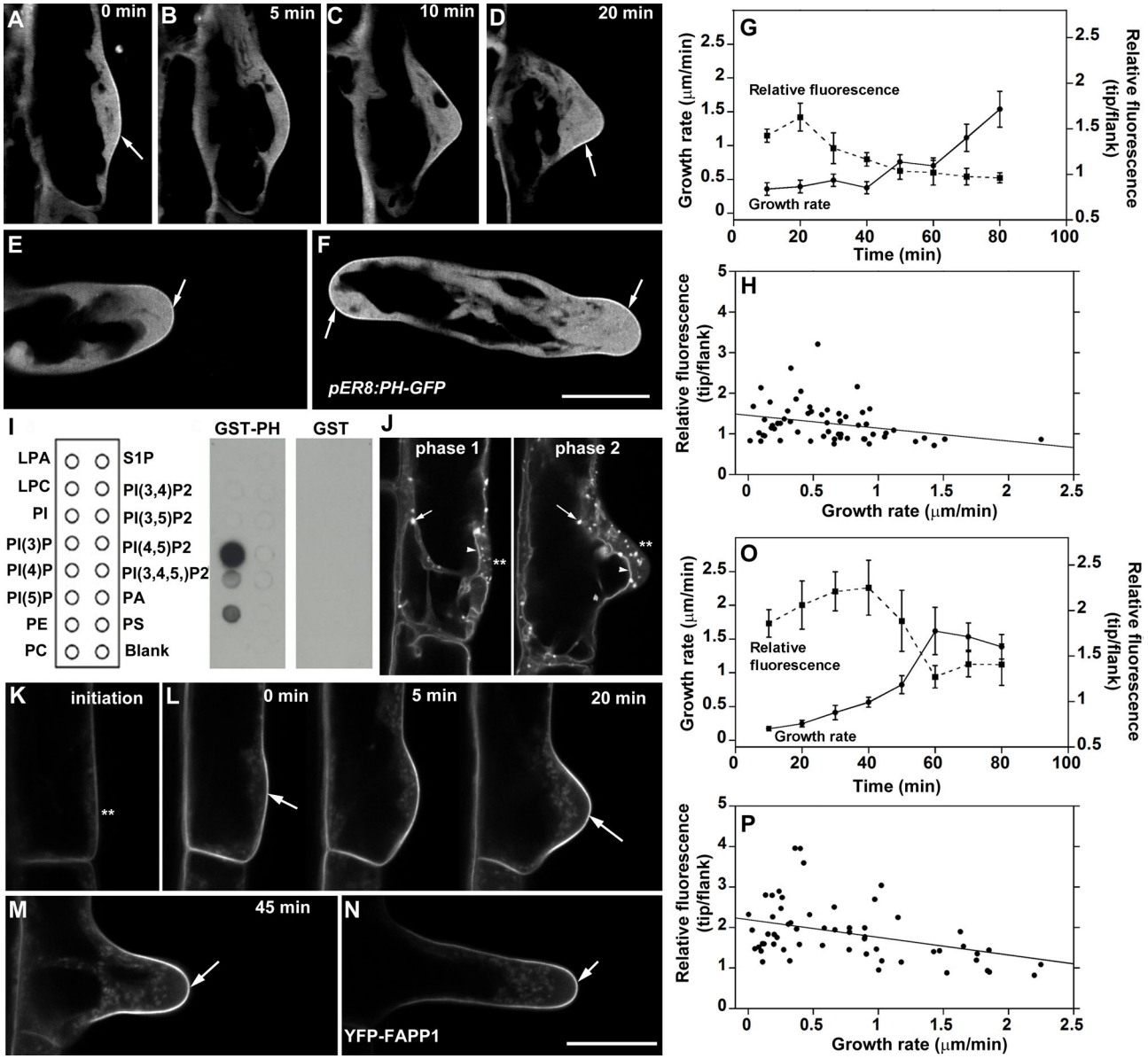

Fig. 7. The PH domain is sufficient for targeting AGD1 to the root hair PM. (A–D) PH-GFP after induction with estradiol marks the PM of phase 1 and phase 2 root hairs (arrows). (E,F) PH-GFP localization to the PM at the apical dome persists in phase 3 root hairs that are bulbous in shape and those that share the same initiation point (arrows). (G,H) Time course (G) and scatter plot (H) of root hair growth rate and PH-GFP tip/flank fluorescence ratio. Pearson's correlation coefficient=−0.284 (*P*=0.030). (I) Protein-lipid overlay assays of strips blotted with various phospholipids. The leftmost panel indicates the positions of phospholipids on the strips. LPA, lysophosphatidic acid; LPC, lysophosphatidylcholine; PE, phosphatidylethanolamine; PC, phosphatidylcholine; S1P, sphingosine-1-P; PI(3,4)P2, phosphatidylinositol 3,4-bisphosphate; PI(3,5)P2, phosphatidylinositol 3,5-bisphosphate; PI(4,5)P2, phosphatidylinositol 4,5-bisphosphate; PI(3,4,5)P2, phosphatidylinositol 3,4,5-bisphosphate; PA, phosphatidic acid; PS, phosphatidylserine. (J) The PI(3)P biosensor YFP-2XFYVE marks endosomes (arrows) and the tonoplast (arrowheads), but not the PM, in phase1 and 2 root hairs. (K,L) The signal of the PI(4)P biosensor, YFP-FAPP1, at the PM is weak at future root hair initiation sites (**) but intensifies in root hairs at phase 1 and 2 (arrows). (M) YFP-FAPP1 broadly labels the PM of a young phase 3 root hair (arrow). (N) In a longer phase 3 root hair, YFP-FAPP1 is enriched at the apical 10 µm of the cell (arrow). (O,P) Time course (O) and scatter plot (P) of root hair growth rate and relative YFP-FAPP1 tip/flank fluorescence. Pearson's correlation coefficient=−0.439 (*P*=0.0005). Scale bars: 20 µm.

at its slowest (i.e. during phase 1, 2 and 4), or when tip growth of rapidly growing phase 3 root hairs are prematurely terminated by hyperosmotic shock. However, the slower root hair growth rate of *agd1* mutants does not fully support the hypothesis that localization of AGD1 to the apical-most region of the root hair limits growth (Yoo et al., 2008). An alternative explanation is that the onset of rapid tip growth results in AGD1 being displaced from the apical-most PM domain of the root hair leading to its accumulation along the lateral PM flanks. The data presented here do not allow us to distinguish between these possibilities and further studies will be needed to better understand how AGD1 dynamics translate to root hair growth status.

To acquire their highly cylindrical shapes and sustain the mostly symmetrical growth typical of tip-growing plant cells, pollen tubes and root hairs direct the nonvectorial internal turgor pressure toward the apical region of the cell through gradients in the stiffness and extensibility of their cell walls. The establishment of these gradients in cell wall stiffness is dictated by endocytic and exocytic trafficking of vesicles to the apical region (Chebli et al., 2013). In pollen tubes, microindentation studies and mathematical modeling have shown

Journal of Cell Science (2018) 131, jcs203828. doi:10.1242/jcs.203828

that apical cell wall stiffness at the tip is less than that of the cylindrical shank allowing turgor-driven expansion of the cell to be confined to the apical-most dome (Zerzour et al., 2009; Fayant et al., 2010). Given their similar growth habits, it is likely that gradients in cell wall biomechanical properties reported for pollen tubes also occur in root hairs. In this regard, depletion of AGD1 at the tip PM as root hairs transition from slow growth in phase 2 to rapid growth in phase 3 suggest that it participates in secretory processes that maintain cell wall softness at the tip while reinforcing cell wall stiffness along the subapical cylindrical shanks (Chebli et al., 2013). Without functional AGD1, it is reasonable to assume that vesicular trafficking at the root hair tip would be altered. A consequence of such a defect in tip-directed trafficking is the development of lateral gradients in cell wall stiffness across opposite flanks of the root hair cell, which in turn would lead to breaking of axial symmetry (Chebli et al., 2013). Broken axial symmetry is evident from the fact that root hairs of *agd1* mutants at phase 3 exhibit wavy/spiral growth and occasional swollen tips, a scenario that can also be explained, in part, by disrupted cytoskeletal organization (Yoo et al., 2008, 2012). Furthermore, our data indicate that enrichment of AGD1 at the apical-most PM domain of root hairs at phase1 and 2 serves to maintain growth at a slow enough rate to ensure stability of the trafficking apparatus as root hairs emerge. The mild apical shift in planar polarity and the formation of two root hair tips from one initiation point in *agd1* mutants support this hypothesis.

The precise mechanism by which AGD1 translates processes occurring at the root hair PM to the establishment of cell wall biomechanical gradients is not known. However, given that AGD1 is an ARF-GAP, a root hair tip-localized ARF-GTPase is likely involved. Although the ARF substrate for AGD1 has yet to be identified, a study showing that overexpression of constitutively active ARF1 was associated with root hair polarity defects in *Arabidopsis* support this possibility (Xu and Scheres, 2005). Furthermore, the observation that BFA, an inhibitor of ARF-GEFs, is capable of reversing the wavy root hair phenotypes of the *agd1* mutant indicates that an ARF-GTPase molecular switching mechanism operates in maintaining normal root hair axial symmetry (Yoo et al., 2008). In addition to ARFs and AGD1, potential components of the ARF-GTPase machinery that drive root hair development are the ARF-GEFs GNOM (also known as GN) and BEN1/MIN7 (Nomura et al., 2006; Tanaka et al., 2009; Naramoto et al., 2010, 2014). Whereas *ben1/min7* mutants were recently shown to exhibit root hair shape defects (Sparks et al., 2016), GNOM and GNOM-like (GNL) ARF-GEFs are required for root hair planar polarity (Fischer et al., 2006). Moreover, GNOM was shown to be involved in root hair tip growth and GNOM-GFP localizes to trichoblasts during early bulge formation, where it is a direct BFA target (Richter et al., 2011; Stanislas et al., 2014).

Our study presents evidence for a critical role of the PH domain in directing AGD1 to the root hair PM based on results showing that an AGD1-GFP fusion with the PH domain deleted (AGD1ΔPH-GFP) was cytosolic, while a GFP fusion to only the PH domain (PH-GFP) still localized to the PM. The importance of the PH domain for TGN/EE localization was also reported for the AGD3 protein (Naramoto et al., 2009). Our results show that the localization of AGD1 to the root hair PM is required for its full functionality as estradiol induction of *AGD1ΔPH-GFP* expression failed to complement the *agd1* root hair phenotypes. However, GAP and ANK domain deletions, despite also maintaining their association with the root hair PM, did not complement the *agd1* root hair phenotypes. In mammalian cells, the ANK and PH domains are required for efficient catalytic activity of multi-domain ARF-GAPs (Ha et al., 2008). The PH domain in particular binds to phosphatidylinositol 4,5-bisphophate [PI(4,5)P2], leading to more efficient ARF-GAP catalytic activity (Ha et al., 2008). Thus, it is possible that, like the GAP domain-deleted fusion, the ANK and PH domain deletions have reduced or no longer possess functional GAP activity. If this is the case, it appears that both the recruitment of AGD1 to the PM and its GAP activity are essential for normal root hair development. We also show that the AGD1 PH domain alone is sufficient for PI monophosphate binding. Like full-length AGD1, the PH domain alone binds to PI(3)P, PI(4)P and PI(5)P (Yoo et al., 2012). Because spatiotemporal patterns of PH-GFP localization to the root hair PM mirrored those of a PI(4)P biosensor (Vermeer et al., 2009), we propose that this PI species is the major phospholipid that recruits AGD1 to the PM. It is worth noting that unlike full-length AGD1-GFP, the PH-GFP fusion persisted at the apical-most PM domain of many phase 3 root hairs. Although one could argue that the persistence of PH-GFP at the root hair PM apex is a consequence of the altered root hair shapes and slower tip growth due to the inability of the construct to complement *agd1*, one cannot discount the possibility that the ANK and GAP domains could be involved in modulating *in planta* binding of the PH domain to specific pools of PI(4)P. This level of interdomain regulation could represent a mechanism for dissociating AGD1 from the apical-most PM domain as root hairs transition to rapid phase 3 tip growth.

The foci decorated by AGD1-GFP did not colocalize with any of the endomembrane markers tested. This result was surprising given that AGD3, a closely related class 1 ARF-GAP, closely localizes to the TGN/EE (Koizumi et al., 2005; Naramoto et al., 2009, 2010). The fact that AGD1-GFP foci are rare or absent in the inducible *pER8:AGD1-GFP*-expressing lines, but yet are able to complement the *agd1* root hair defects, suggests that AGD1 at the PM, rather than those at the foci, are crucial for maintaining polar root hair growth. Although our observations imply that the AGD1-GFP bodies are possibly mislocalization artifacts, we cannot discount the possibility that they represent unknown organelles. Additional tools, including colocalizing AGD1-GFP with other red-emitting endomembrane markers not represented in our study and immunoelectron microscopy of high pressure-frozen root samples, are needed to determine if these AGD1-GFP foci reflect the authentic localization of native AGD1.

In summary, our work sheds new light on the role of an ACAP-type ARF-GAP in plants and highlights the advantages of the root hair system as a model for addressing basic cell biological questions. Based on our results, we propose that differential recruitment of AGD1 to specific PM domains during root hair development is a process that is pivotal for its *in vivo* function. When associated with the PM, AGD1 restricts growth in bulging root hairs and those that are at an early stage of development. Maintaining tip growth at this slower, restricted pace stabilizes the trafficking apparatus to ensure normal root hair emergence. By dissipating from the tip PM, this AGD1-imposed growth restriction is released, allowing root hairs to grow at a more rapid rate while maintaining symmetrical growth. Finally, our study shows that tight control of spatiotemporal patterns of AGD1 localization is facilitated, in part, through the association of its PH domain with pools of tip-enriched PI(4)P.

MATERIALS AND METHODS

Generation of *AGD1pro* and estradiol-inducible *AGD1-GFP* and deletion constructs

The *AGD1* promoter was amplified using the primers $AGD1_{pro}$ *F* and $AGD1_{pro}$*R*. The polymerase chain reaction (PCR) product was cloned to the pDONRP4-P1R vector (Invitrogen) by the Gateway BP reaction. For the

Journal of Cell Science (2018) 131, jcs203828. doi:10.1242/jcs.203828

AGD1 open reading frame (ORF), the primers *AGD1F* and *AGD1R* were used to amplify the *AGD1* gene and clone it to the pENTR D-Topo vector (Invitrogen). *Arabidopsis* genomic DNA isolated from 10-day-old seedlings was used as a template for the PCR reaction. The *AGD1pro:AGD1-GFP* fusion construct was generated by incorporating the *AGD1* promoter and *AGD1* ORF entry clones into the R4pGWB450 vector through the LR reaction (Nakagawa et al., 2008).

AGD1-GFP deletion constructs were generated using the estradiol-inducible expression vector pER8 (Zuo et al., 2000). Complementary DNA (cDNA) of *AGD1* was amplified from 10-day-old seedlings by PCR using primers AGD1-XhoI-F/AGD1-SpeI-R and cloned into *pER8*. The g3GFP DNA fragment was amplified using *AGD1pro:AGD1-GFP* as a template and fused to the SpeI site at the C-terminus of AGD1 to generate *pER8:AGD1-GFP*. To generate the AGD1 deletion constructs, a similar strategy was used. In the case of *pER8:AGD1ΔPH-GFP*, for example, the N-terminal BAR domain and the C-terminal GAP-ANK domains of AGD1 were amplified using primers AGD1-XhoI-F/268-EcoRI-R and 457-EcoRI-F/AGD1-SpeI-R, respectively. The two DNA fragments were sequentially cloned into the pBluescript II vector. The resulting DNA was then cloned into the XhoI/SpeI sites of the pER8 vector, and the g3GFP fragment was fused into the SpeI site at the C-terminus. Primers used to generate the constructs are shown in Table S1.

The *agd1-1* mutant (Yoo et al., 2008) was transformed with $AGD1_{pro}$*:AGD1-GFP* and inducible *pER8* constructs using the floral dip method (Clough and Bent, 1998). Antibiotic-resistant seedlings with GFP signal were selected using an SZX12 stereofluorescence microscope (Olympus America).

Imaging of AGD1-GFP in living roots

Arabidopsis seeds were sterilized with 95% (v/v) ethanol and 20% (v/v) bleach. Seeds were planted on 0.5% phyta-agar supplemented with half strength Murashige and Skoog (MS) salts, 1% sucrose, and the vitamins pyridoxine-HCl (0.5 mg/ml), nicotinic acid (0.5 mg/ml) and thiamine (1 mg/ml), layered onto 48×64 mm cover slips as detailed in Dyachok et al. (2016). Coverslips were placed in 90 mm Petri dishes and positioned at a 20° angle from the vertical, under a 14 h-light–10 h-dark cycle at 22°C to allow primary roots to grow along the surface of the coverslips. Five days after planting, coverslips containing the seedlings were transferred to the stage of an UltraView ERS spinning disc confocal microscope (Perkin-Elmer Life and Analytical Sciences) or an SP8 X point scanning confocal microscope (Leica Microsystems) equipped with 40× or 63× water-immersion objectives. GFP was excited using the 488-nm line of the argon laser, and emission was detected at 510 nm. For lines expressing the *pER8*-inducible constructs, MS medium containing 10–20 µM estradiol was applied directly to seedling roots using a 10 ml syringe. Seedlings were observed 24 h after induction.

Time-lapse sequences and single time point images were captured using the spinning disc confocal microscope running Improvision Volocity acquisition software version 5.4.2 (Perkin Elmer) or the SP8 X running LAS AF software (Leica Microsystems). Root hair images were obtained at a fixed focal plane that spanned the median of the cell. For time-lapse microscopy, images were captured every 1 s for 1 min. To analyze expression patterns in primary roots of *AGD1pro: AGD1-GFP* lines, a series of optical sections were taken at 0.5 µm intervals and merged using the isosurface rendering function of Volocity 5.4.2 visualization software (Perkin Elmer).

Root hair growth rates from lines expressing AGD1-GFP, PH-GFP and YFP-FAPP1 were obtained by capturing single optical confocal images from trichoblasts every 10 min for 80 min. Images corresponding to the first time points were captured from root hair bulges that were 2–5 µm in length. Root hair growth rate expressed as µm/min was calculated by first measuring the displacement of the root hair tip overtime for every 10 min time point and dividing this number by 10. AGD1-GFP, PH-GFP and YFP-FAPP1 fluorescence was quantified from the same root hairs in which growth rate was measured. A 2 pixel line ∼10 µm in length was drawn along the root hair cell edges that corresponded to the PM of the tip and flanks (see inset in Fig. 3K), and average fluorescence intensity was acquired using Image J (https://imagej.nih.gov/ij/). The ratio of average tip and flank fluorescence intensity was obtained, and presented as relative fluorescence.

Colocalization of AGD1-GFP foci with mCherry endomembrane markers

AGD1pro: AGD1-GFP lines were crossed with plants expressing the WAVE-mCherry collection of membrane markers (Geldner et al., 2009) or directly transformed with *mCherry-G-rk* Golgi (Nelson et al., 2007) and ARA6-mCherry constructs. The mCherry-Golgi and WAVE lines were obtained from the Arabidopsis Biological Research Center (Columbus, OH). The ARA6-mCherry construct was made by subcloning into a pCAMBIA1390 vector that had the *cauliflower mosaic virus* (*35S*) promoter. Full-length *ARA6* was amplified from genomic DNA from 10-day-old seedlings using the primers *ARA6-SalI-F* and *ARA6-BamHI-R* (Table S1). Plants emitting both green and red fluorescence were selected under a stereo fluorescence microscope and propagated for seed. Seedlings were imaged using the sequential scanning mode of the SP8 X confocal microscope.

Lipid overlay assays

The PH domain, which spanned 867–1281 base pairs of the *AGD1* gene, was PCR amplified from cDNA obtained from 10-day-old seedlings with gene-specific primers *AGD1-PH-BamH1-F* and *AGD1-PH-Sal1-R* (Table S1). The PCR product was cloned into the pGEX5X-1 GST vector at the BamH1 and Sal1 sites. For protein expression, the construct was transformed into BL21 cells and grown in 5 ml Luria-Bertani (LB) broth (Thermo Fisher Scientific) overnight at 37°C. The culture was induced with 1 mM isopropyl-β-D-thiogalactopyranoside (IPTG) (Thermo Fisher Scientific) and incubated for an additional 3 h. Cells were then lysed and proteins purified by incubation in GST resin (Qiagen). Proteins were resolved on a polyacrylamide gel and detected by Coomassie staining. For the lipid overlay assays, ∼2.5 µg GST or GST-PH proteins were incubated with the PI membranes (Echelon Biosciences) at 4°C overnight, and bound proteins were detected with anti-GST HRP-conjugated antibody (Abcam).

Statistical analysis

All values are expressed as mean±standard error of the mean (s.e.m.). Measurements were obtained from at least four independent experiments with 10 seedlings per experiment. One-way analysis of variance (ANOVA) followed by post hoc Tukey's Honestly Significant Difference (HSD) test (SPSS version 23) were used to determine statistical differences among means. For determining differences in root hair planar polarity, the nonparametric Kolmogorov–Smirnov test was used to test the null hypothesis that distribution of relative root hair position between two genotypes (e.g. wild type versus *agd1*) are similar. The null hypothesis was rejected if $P<0.01$. A total of 178 cells from ∼30 seedlings were measured. To determine the relationship between root hair growth rate and AGD1-GFP, PH-GFP or YFP-FAPP1 fluorescence, Pearson's correlation analysis was used. The inverse relationship between root hair growth rate and tip/flank fluorescence was determined to be statistically significant if $P\neq0$ based on 120 pairwise measurements.

Acknowledgements

We thank Soonil Kwon for assistance with the statistical analysis.

Competing interests

The authors declare no competing or financial interests.

Author contributions

Conceptualization: C.-M.Y., S.N., H.F., E.B.B.; Methodology: C.-M.Y., S.N., J.A.S., B.R.K., J.N., E.B.B.; Validation: C.-M.Y., J.A.S., E.B.B.; Formal analysis: C.-M.Y., J.A.S., J.N., E.B.B.; Investigation: C.-M.Y., B.R.K., J.N., E.B.B.; Resources: C.-M.Y., S.N., B.R.K., H.F., E.B.B.; Writing - original draft: E.B.B.; Writing - review & editing: C.-M.Y., S.N., J.A.S., B.R.K., J.N., E.B.B.; Supervision: H.F., E.B.B.; Project administration: E.B.B.; Funding acquisition: S.N., E.B.B.

Funding

This work was supported by the Noble Research Institute and National Aeronautics and Space Administration (NNX12AM94G to E.B.B.). S.N. was supported by a Tomizawa Jun-ichi and Keiko Fund.

Supplementary information

Supplementary information available online at
http://jcs.biologists.org/lookup/doi/10.1242/jcs.203828.supplemental

References

Bernal, A. J., Yoo, C.-M., Mutwil, M., Jensen, J. K., Hou, G., Blaukopf, C., Sørensen, I., Blancaflor, E. B., Scheller, H. V. and Willats, W. G. T. (2008). Functional analysis of the cellulose synthase-like genes CSLD1, CSLD2, and CSLD4 in tip-growing arabidopsis cells. *Plant Physiol.* **148**, 1238-1253.

Böhme, K., Li, Y., Charlot, F., Grierson, C., Marrocco, K., Okada, K., Laloue, M. and Nogué, F. (2004). The Arabidopsis COW1 gene encodes a phosphatidylinositol transfer protein essential for root hair tip growth. *Plant J.* **40**, 686-698.

Brown, L. K., George, T. S., Thompson, J. A., Wright, G., Lyon, J., Dupuy, L., Hubbard, S. F. and White, P. J. (2012). What are the implications of variation in root hair length on tolerance to phosphorus deficiency in combination with water stress in barley (Hordeum vulgare)? *Ann. Bot.* **110**, 319-328.

Brown, L. K., George, T. S., Dupuy, L. X. and White, P. J. (2013). A conceptual model of root hair ideotypes for future agricultural environments: what combination of traits should be targeted to cope with limited P availability? *Ann. Bot.* **112**, 317-330.

Carol, R. J., Takeda, S., Linstead, P., Durrant, M. C., Kakesova, H., Derbyshire, P., Drea, S., Zarsky, V. and Dolan, L. (2005). A RhoGDP dissociation inhibitor spatially regulates growth in root hair cells. *Nature* **438**, 1013-1016.

Chebli, Y., Kroeger, J. and Geitmann, A. (2013). Transport logistics in pollen tubes. *Mol. Plant* **6**, 1037-1052.

Clough, S. J. and Bent, A. F. (1998). Floral dip: a simplified method for *Agrobacterium*-mediated transformation of *Arabidopsis thaliana*. *Plant J.* **16**, 735-743.

D'Souza-Schorey, C. and Chavrier, P. (2006). ARF proteins: roles in membrane traffic and beyond. *Nat. Rev. Mol. Cell Biol.* **7**, 347-358.

Dolan, L., Duckett, C. M., Grierson, C., Linstead, P., Schneider, K., Lawson, E., Dean, C., Poethig, S. and Roberts, K. (1994). Clonal relationships and cell patterning in the root epidermis of Arabidopsis. *Development* **120**, 2465-2474.

Donaldson, J. G. and Jackson, C. L. (2011). ARF family G proteins and their regulators: roles in membrane transport, development and disease. *Nat. Rev. Mol. Cell Biol.* **12**, 362-375.

Dyachok, J., Paez-Garcia, A., Yoo, C.-M., Palanichelvam, K. and Blancaflor, E. B. (2016). Fluorescence imaging of the cytoskeleton in plant roots. *Methods Mol. Biol.* **1365**, 139-153.

East, M. P. and Kahn, R. A. (2011). Models for the functions of Arf GAPs. *Sem. Cell Dev. Biol.* **22**, 3-9.

Favery, B., Ryan, E., Foreman, J., Linstead, P., Boudonck, K., Steer, M., Shaw, P. and Dolan, L. (2001). KOJAK encodes a cellulose synthase-like protein required for root hair cell morphogenesis in Arabidopsis. *Genes Dev.* **15**, 79-89.

Fayant, P., Girlanda, O., Chebli, Y., Aubin, C.-É., Villemure, I. and Geitmann, A. (2010). Finite element model of polar growth in pollen tubes. *Plant Cell* **22**, 2579-2593.

Fischer, U., Ikeda, Y., Ljung, K., Serralbo, O., Singh, M., Heidstra, R., Palme, K., Scheres, B. and Grebe, M. (2006). Vectorial information for arabidopsis planar polarity is mediated by combined AUX1, EIN2, and GNOM activity. *Curr. Biol.* **16**, 2143-2149.

Foreman, J., Demidchik, V., Bothwell, J. H. F., Mylona, P., Miedema, H., Torres, M. A., Linstead, P., Costa, S., Brownlee, C., Jones, J. D. G. et al. (2003). Reactive oxygen species produced by NADPH oxidase regulate plant cell growth. *Nature* **422**, 442-446.

Geldner, N., Dénervaud-Tendon, V., Hyman, D. L., Mayer, U., Stierhof, Y.-D. and Chory, J. (2009). Rapid, combinatorial analysis of membrane compartments in intact plants with a multicolor marker set. *Plant J.* **59**, 169-178.

Gillingham, A. K. and Munro, S. (2007). The small G proteins of the Arf family and their regulators. *Annu. Rev. Cell Dev. Biol.* **23**, 579-611.

Grierson, C. S., Parker, J. S. and Kemp, A. C. (2001). Arabidopsis genes with roles in root hair development. *J. Plant Nutr. Soil Sci.* **164**, 131-140.

Grierson, C., Nielsen, E., Ketelaarc, T. and Schiefelbein, J. (2014). Root hairs. *Arabidopsis Book* **12**, e0172.

Ha, V. L., Luo, R., Nie, Z. and Randazzo, P. A. (2008). Contribution of AZAP-type Arf GAPs to cancer cell migration and invasion. *Adv. Cancer Res.* **101**, 1-28.

Hemsley, P. A., Kemp, A. C. and Grierson, C. S. (2005). The TIP GROWTH DEFECTIVE1 S-Acyl transferase regulates plant cell growth in arabidopsis. *Plant Cell* **17**, 2554-2563.

Inoue, H. and Randazzo, P. A. (2007). Arf GAPs and their interacting proteins. *Traffic* **8**, 1465-1475.

Jackson, T. R., Brown, F. D., Nie, Z., Miura, K., Foroni, L., Sun, J., Hsu, V. W., Donaldson, J. G. and Randazzo, P. A. (2000). Acaps are Arf6 Gtpase-activating proteins that function in the cell periphery. *J. Cell Biol.* **151**, 627-638.

Jensen, R. B., Lykke-Andersen, K., Frandsen, G. I., Nielsen, H. B., Haseloff, J., Jespersen, H. M., Mundy, J. and Skriver, K. (2000). Promiscuous and specific phospholipid binding by domains in ZAC, a membrane-associated Arabidopsis protein with an ARF GAP zinc finger and a C2 domain. *Plant Mol. Biol.* **44**, 799-814.

Jones, M. A., Shen, J.-J., Fu, Y., Li, H., Yang, Z. and Grierson, C. S. (2002). The arabidopsis Rop2 GTPase is a positive regulator of both root hair initiation and tip growth. *Plant Cell* **14**, 763-776.

Kobayashi, H. and Fukuda, M. (2012). Rab35 regulates Arf6 activity through centaurin-β2 (ACAP2) during neurite outgrowth. *J. Cell Sci.* **125**, 2235-2243.

Kobayashi, H. and Fukuda, M. (2013). Arf6, Rab11 and transferrin receptor define distinct populations of recycling endosomes. *Commun. Integr. Biol.* **6**, e25036.

Koizumi, K., Naramoto, S., Sawa, S., Yahara, N., Ueda, T., Nakano, A., Sugiyama, M. and Fukuda, H. (2005). VAN3 ARF–GAP-mediated vesicle transport is involved in leaf vascular network formation. *Development* **132**, 1699-1711.

Kusano, H., Testerink, C., Vermeer, J. E. M., Tsuge, T., Shimada, H., Oka, A., Munnik, T. and Aoyama, T. (2008). The *Arabidopsis* phosphatidylinositol phosphate 5-kinase PIP5K3 is a key regulator of root hair tip growth. *Plant Cell* **20**, 367-380.

Lai, Y.-S., Stefano, G. and Brandizzi, F. (2014). ER stress signaling requires RHD3, a functionally conserved ER-shaping GTPase. *J. Cell Sci.* **127**, 3227-3232.

Lemmon, M. A., Ferguson, K. M. and Schlessinger, J. (1996). PH domains: diverse sequences with a common fold recruit signaling molecules to the cell surface. *Cell* **85**, 621-624.

Liljegren, S. J., Leslie, M. E., Darnielle, L., Lewis, M. W., Taylor, S. M., Luo, R., Geldner, N., Chory, J., Randazzo, P. A., Yanofsky, M. F. et al. (2009). Regulation of membrane trafficking and organ separation by the NEVERSHED ARF-GAP protein. *Development* **136**, 1909-1918.

Min, M. K., Kim, S. J., Miao, Y., Shin, J., Jiang, L. and Hwang, I. (2007). Overexpression of arabidopsis AGD7 causes relocation of golgi-localized proteins to the endoplasmic reticulum and inhibits protein trafficking in plant cells. *Plant Physiol.* **143**, 1601-1614.

Molendijk, A. J., Bischoff, F., Rajendrakumar, C. S. V., Friml, J., Braun, M., Gilroy, S. and Palme, K. (2001). Arabidopsis thaliana Rop GTPases are localized to tips of root hairs and control polar growth. *EMBO J.* **20**, 2779-2788.

Müller, M. P. and Goody, R. S. (2017). Molecular control of Rab activity by GEFs, GAPs and GDI. *Small GTPases* 1-17.

Nakagawa, T., Nakamura, S., Tanaka, K., Kawamukai, M., Suzuki, T., Nakamura, K., Kimura, T. and Ishiguro, S. (2008). Development of R4 gateway binary vectors (R4pGWB) enabling high-throughput promoter swapping for plant research. *Biosci. Biotechnol. Biochem.* **72**, 624-629.

Naramoto, S., Sawa, S., Koizumi, K., Uemura, T., Ueda, T., Friml, J., Nakano, A. and Fukuda, H. (2009). Phosphoinositide-dependent regulation of VAN3 ARF-GAP localization and activity essential for vascular tissue continuity in plants. *Development* **136**, 1529-1538.

Naramoto, S., Kleine-Vehn, J., Robert, S., Fujimoto, M., Dainobu, T., Paciorek, T., Ueda, T., Nakano, A., Van Montagu, M. C. E., Fukuda, H. et al. (2010). ADP-ribosylation factor machinery mediates endocytosis in plant cells. *Proc. Natl. Acad. Sci. USA* **107**: 21890-21895.

Naramoto, S., Otegui, M. S., Kutsuna, N., de Rycke, R., Dainobu, T., Karampelias, M., Fujimoto, M., Feraru, E., Miki, D., Fukuda, H. et al. (2014). Insights into the localization and function of membrane trafficking regulator GNOM ARF-GEF at the Golgi apparatus in Arabidopsis. *Plant Cell* **26**, 3062-3076.

Nelson, B. K., Cai, X. and Nebenführ, A. (2007). A multicolored set of in vivo organelle markers for co-localization studies in Arabidopsis and other plants. *Plant J.* **51**, 1126-1136.

Nomura, K., Debroy, S., Lee, Y. H., Pumplin, N., Jones, J. and He, S. Y. (2006). A bacterial virulence protein suppresses host innate immunity to cause plant disease. *Science* **313**, 220-223.

Park, E. and Nebenführ, A. (2013). Myosin XIK of arabidopsis thaliana accumulates at the root hair tip and is required for fast root hair growth. *PLoS ONE* **8**, e76745.

Park, S., Szumlanski, A. L., Gu, F., Guo, F. and Nielsen, E. (2011). A role for CSLD3 during cell-wall synthesis in apical plasma membranes of tip-growing root-hair cells. *Nat. Cell Biol.* **13**, 973-980.

Parker, J. S., Cavell, A. C., Dolan, L., Roberts, K. and Grierson, C. S. (2000). Genetic interactions during root hair morphogenesis in arabidopsis. *Plant Cell* **12**, 1961-1974.

Richter, S., Müller, L. M., Stierhof, Y.-D., Mayer, U., Takada, N., Kost, B., Vieten, A., Geldner, N., Koncz, C. and Jürgens, G. (2011). Polarized cell growth in Arabidopsis requires endosomal recycling mediated by GBF1-related ARF exchange factors. *Nat. Cell Biol.* **14**, 80-86.

Robinson, D. G., Jiang, L. and Schumacher, K. (2008). The endosomal system of plants: charting new and familiar territories. *Plant Physiol.* **147**, 1482-1492.

Rounds, C. M. and Bezanilla, M. (2013). Growth mechanisms in tip-growing plant cells. *Annu. Rev. Plant Biol.* **64**, 243-265.

Salazar-Henao, J. E. and Schmidt, W. (2016). An inventory of nutrient-responsive genes in arabidopsis root hairs. *Front Plant Sci* **7**, 237.

Schiefelbein, J. W. and Somerville, C. (1990). Genetic control of root hair development in arabidopsis thaliana. *Plant Cell* **2**, 235-243.

Seifert, G. J., Barber, C., Wells, B., Dolan, L. and Roberts, K. (2002). Galactose biosynthesis in arabidopsis: genetic evidence for substrate channeling from UDP-D-galactose into cell wall polymers. *Curr. Biol.* **12**, 1840-1845.

Sieburth, L. E., Muday, G. K., King, E. J., Benton, G., Kim, S., Metcalf, K. E., Meyers, L., Seamen, E. and Van Norman, J. M. (2006). SCARFACE encodes an

ARF-GAP that is required for normal auxin efflux and vein patterning in arabidopsis. *Plant Cell* **18**, 1396-1411.
Song, X.-F., Yang, C.-Y., Liu, J. and Yang, W.-C. (2006). RPA, a class II ARFGAP protein, activates ARF1 and U5 and plays a role in root hair development in arabidopsis. *Plant Physiol.* **141**, 966-976.
Sparks, J. A., Kwon, T., Renna, L., Liao, F., Brandizzi, F. and Blancaflor, E. B. (2016). HLB1 is a tetratricopeptide repeat domain-containing protein that operates at the intersection of the exocytic and endocytic pathways at the TGN/EE in arabidopsis. *Plant Cell* **28**, 746-769.
Stanislas, T., Grebe, M. and Boutté, Y. (2014). Sterol dynamics during endocytic trafficking in arabidopsis. In *Plant Endosomes: Methods and Protocols* (ed. M.S. Otegui), pp. 13-29. New York, NY: Springer New York.
Stanislas, T., Hüser, A., Barbosa, I. C. R., Kiefer, C. S., Brackmann, K., Pietra, S., Gustavsson, A., Zourelidou, M., Schwechheimer, C. and Grebe, M. (2015). Arabidopsis D6PK is a lipid domain-dependent mediator of root epidermal planar polarity. *Nat. Plants* **1**, 15162.
Stefano, G., Renna, L., Rossi, M., Azzarello, E., Pollastri, S., Brandizzi, F., Baluska, F. and Mancuso, S. (2010). AGD5 is a GTPase-activating protein at the trans-Golgi network. *Plant J.* **64**, 790-799.
Stenzel, I., Ischebeck, T., König, S., Hołubowska, A., Sporysz, M., Hause, B. and Heilmann, I. (2008). The type B phosphatidylinositol-4-phosphate 5-kinase 3 is essential for root hair formation in *Arabidopsis thaliana*. *Plant Cell* **20**, 124-141.
Tanaka, H., Kitakura, S., De Rycke, R., De Groodt, R. and Friml, J. (2009). Fluorescence imaging-based screen identifies ARF GEF component of early endosomal trafficking. *Curr. Biol.* **19**, 391-397.
Thole, J. M., Vermeer, J. E. M., Zhang, Y., Gadella, T. W. J. and Nielsen, E. (2008). ROOT HAIR DEFECTIVE4 Encodes a Phosphatidylinositol-4-Phosphate Phosphatase Required for Proper Root Hair Development in Arabidopsis thaliana. *Plant Cell* **20**, 381-395.
Vermeer, J. E. M., van Leeuwen, W., Tobeña-Santamaria, R., Laxalt, A. M., Jones, D. R., Divecha, N., Gadella, T. W. J. and Munnik, T. (2006). Visualization of PtdIns3P dynamics in living plant cells. *Plant J.* **47**, 687-700.
Vermeer, J. E. M., Thole, J. M., Goedhart, J., Nielsen, E., Munnik, T. and Gadella, T. W. J.Jr (2009). Imaging phosphatidylinositol 4-phosphate dynamics in living plant cells. *Plant J.* **57**: 356-372.
Vernoud, V., Horton, A. C., Yang, Z. and Nielsen, E. (2003). Analysis of the small GTPase gene superfamily of arabidopsis. *Plant Physiol.* **131**, 1191-1208.
Wang, X., Cnops, G., Vanderhaeghen, R., De Block, S., Van Montagu, M. and Van Lijsebettens, M. (2001). AtCSLD3, a cellulose synthase-like gene important for root hair growth in arabidopsis. *Plant Physiol.* **126**, 575-586.
Wang, J., Cai, Y., Miao, Y., Lam, S. K. and Jiang, L. (2009). Wortmannin induces homotypic fusion of plant prevacuolar compartments. *J. Exp. Bot.* **60**, 3075-3083.
Wang, H., Tse, Y. C., Law, A. H. Y., Sun, S. S. M., Sun, Y.-B., Xu, Z.-F., Hillmer, S., Robinson, D. G. and Jiang, L. (2010). Vacuolar sorting receptors (VSRs) and secretory carrier membrane proteins (SCAMPs) are essential for pollen tube growth. *Plant J.* **61**, 826-838.
Xu, J. and Scheres, B. (2005). Dissection of arabidopsis ADP-RIBOSYLATION FACTOR 1 function in epidermal cell polarity. *Plant Cell* **17**, 525-536.
Yoo, C.-M. and Blancaflor, E. (2013). Overlapping and divergent signaling pathways for ARK1 and AGD1 in the control of root hair polarity in Arabidopsis thaliana. *Front Plant Sci.* **4**, 528.
Yoo, C.-M., Wen, J., Motes, C. M., Sparks, J. A. and Blancaflor, E. B. (2008). A class I ADP-Ribosylation factor GTPase-activating protein is critical for maintaining directional root hair growth in arabidopsis. *Plant Physiol.* **147**, 1659-1674.
Yoo, C.-M., Quan, L., Cannon, A. E., Wen, J. and Blancaflor, E. B. (2012). AGD1, a class 1 ARF-GAP, acts in common signaling pathways with phosphoinositide metabolism and the actin cytoskeleton in controlling Arabidopsis root hair polarity. *Plant J.* **69**, 1064-1076.
Zerzour, R., Kroeger, J. and Geitmann, A. (2009). Polar growth in pollen tubes is associated with spatially confined dynamic changes in cell mechanical properties. *Dev. Biol.* **334**, 437-446.
Zuo, J., Niu, Q.-W. and Chua, N.-H. (2000). An estrogen receptor-based transactivator XVE mediates highly inducible gene expression in transgenic plants. *Plant J.* **24**, 265-273.

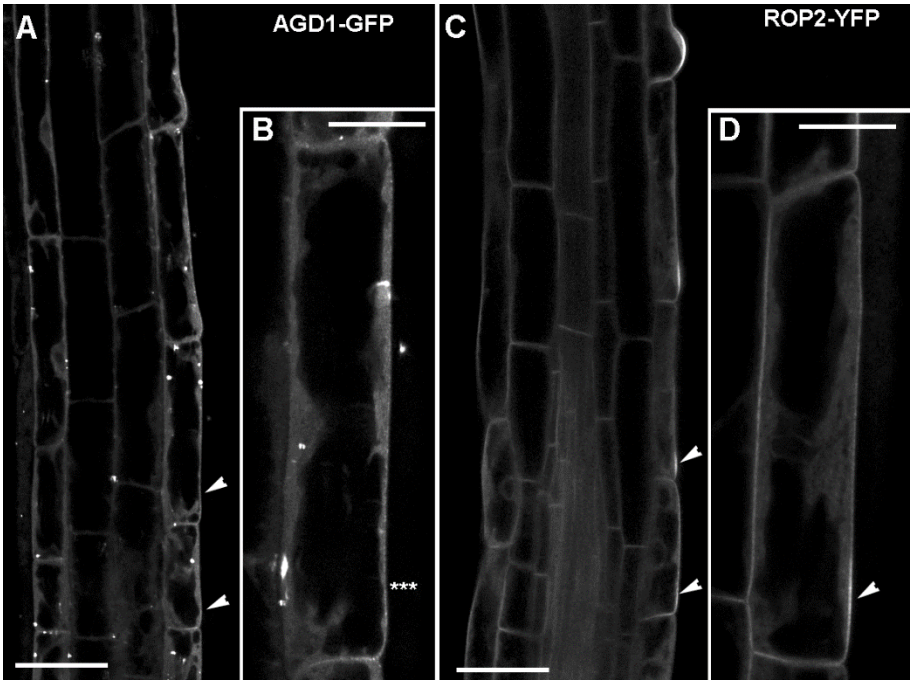

Fig. S1. AGD1 marks the plasma membrane at the root hair initiation site later than ROP2. (A, B) No obvious AGD1-GFP signal can be detected at future root hair initiation sites in trichoblasts (arrowheads in A and asterisks *** in B) in the root elongation zone. (C, D) ROP2-YFP signal accumulates at the plasma membrane of future root hair initiation sites (arrowheads in C, D) much earlier than AGD1-GFP. Bars = 50 μm (A,C); 20 μm (B,D).

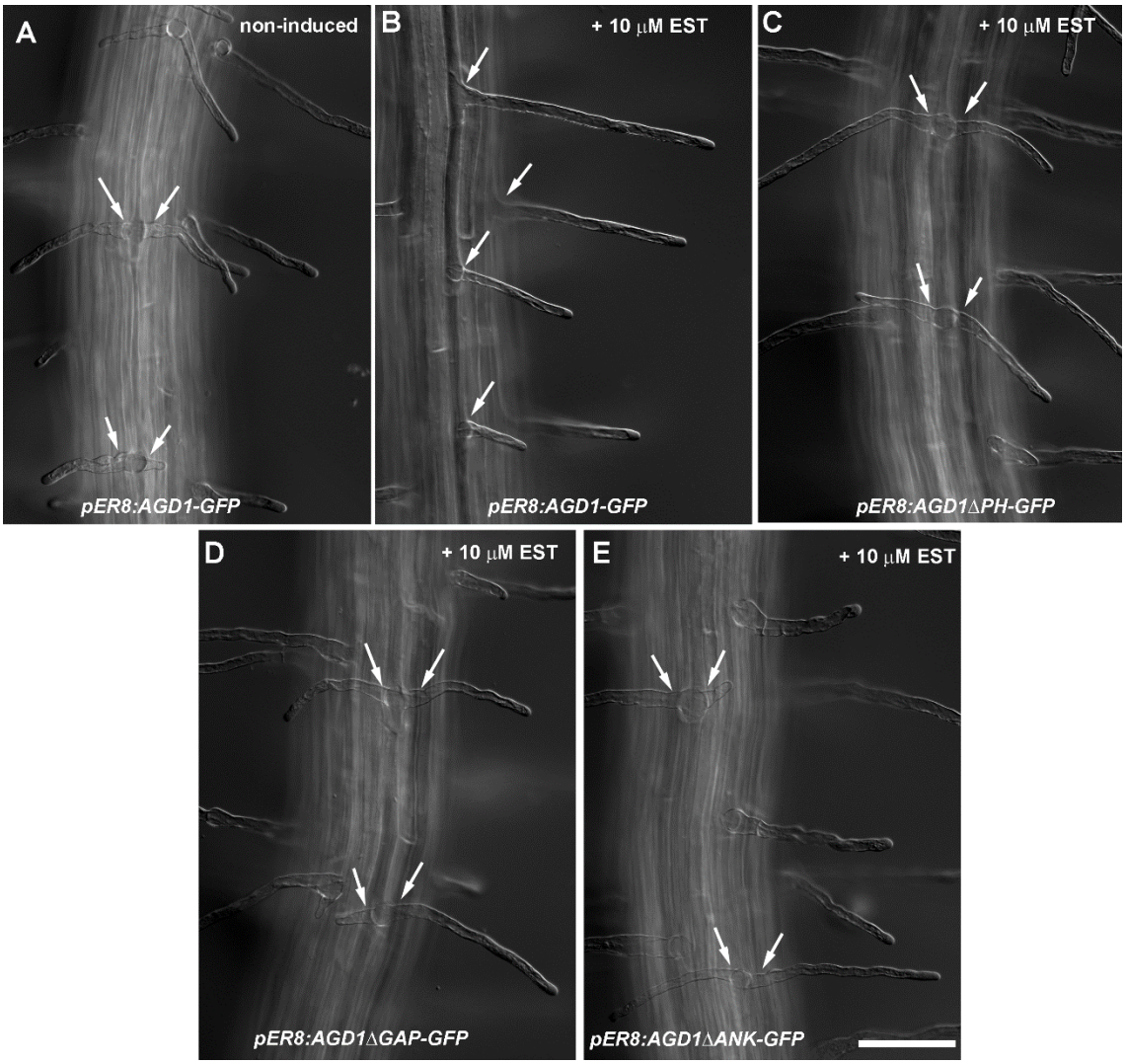

Fig. S2. Domain-deleted AGD1-GFP variants do not complement root hair defects of *agd1*. (A) Root hairs of non-induced *agd1* expressing *pER:AGD1-GFP* show the two tip from one initiation point phenotype (arrows). (B) 24 h after estradiol (EST) application, root hairs of *pER8:AGD1-GFP*-expressing lines have only one root hair per initiation site similar to wild type (arrows). (C-E). None of the AGD1- domain-deleted variants are rescued by EST treatment. Bars = 50 μm.

Table S1. Primer names and sequence used for generating constructs.

Primer	Sequence
AGD1$_{pro}$ F	GGGGACAACTTTGTATAGAAAAGTTGGACCGGGATTATGGAGGAAGAGAGGGCTCC
AGD1$_{pro}$ R	GGGGACTGCTTTTTTGTACAAACTTGATCGTCTGCGGGAAAAGAAAGAGACGGAGAAG
AGD1F	CACCATGCATTTCGCCAAGCTCGATGATTC
AGD1R	TCTTTTGGAGTCTGTTAATAAAGCAATC
AGD1-XhoI-F	ACTCGAGATGCATTTCGCCAAGCTCGATGATTC
AGD1-SpeI-R	AGACTAGTTCTTTTGGAGTCTGTTAATAAAGC
g3GFP-F	AGACTAGTGGTGGCGGAAGCGGAGGCGGTAG
g3GFP-R	AGACTAGTTTATTTGTATAGTTCATCCATGC
268-EcoRI-R	CTGAATTCTGAGTTATGTCTCATGCCATC
460-EcoRI-R	CTGAATTCAGGATCTGCTAAAGAACCAG
457-EcoRI-F	CTGAATTCTTAGCAGATCCTTATGATATCG
641-EcoRI-F	CTGAATTCGACAGTCAGCATTTTCAGGCAG
241-XhoI-F	ACTCGAGATGCAGGAATACCAAAGGCAAG
641-XhoI-F	ACTCGAGATGGACAGTCAGCATTTTCAGGCAG
460-SpeI-R	AGACTAGTAGGATCTGCTAAAGAACCAG
661-SpeI-R	AGACTAGTCTTGTCGTTGGCACGGACATTC
ARA6-SalI-F	GTTGTCGACATGGGATGTGCTTCTTCTCTTCCAG
ARA6-BamHI-R	GTGGATCCTGTGACGAAGGAGCAGGACGAGGTAG
AGD1-PH-BamH1-F	GGATCCAGTTGTGAATTGTGTTCCAGAGC
AGD1-PH-Sal1-R	GTCGACAATAGCAACCGGACGCAGCTGG

Movies

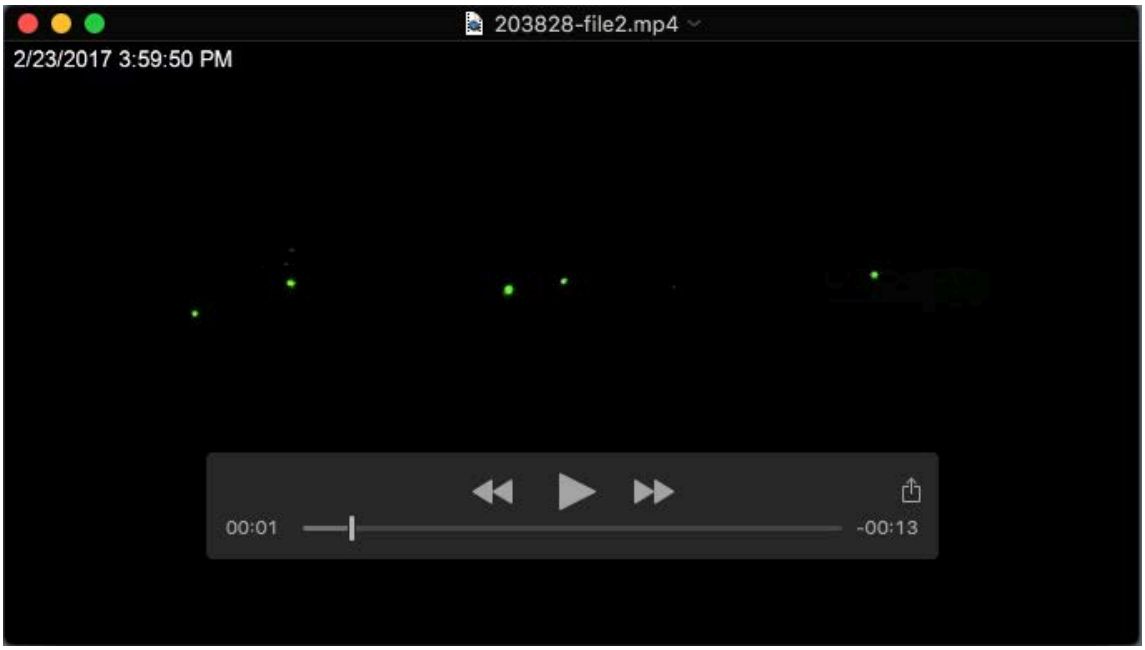

Movie 1. Time-lapse imaging of AGD1-GFP foci in a living phase 3 root hair. Images were taken at a single plane of focus every 1 sec for about 1 minute with a point scanning confocal microscope.

Journal of Cell Science • Supplementary information

Movie 2. Spinning-disc confocal microscopy of AGD1-GFP foci and RabA1g-mCherry (TGN/EE marker) in a living phase 3 root hair. Total elapsed time is about 1 minute.

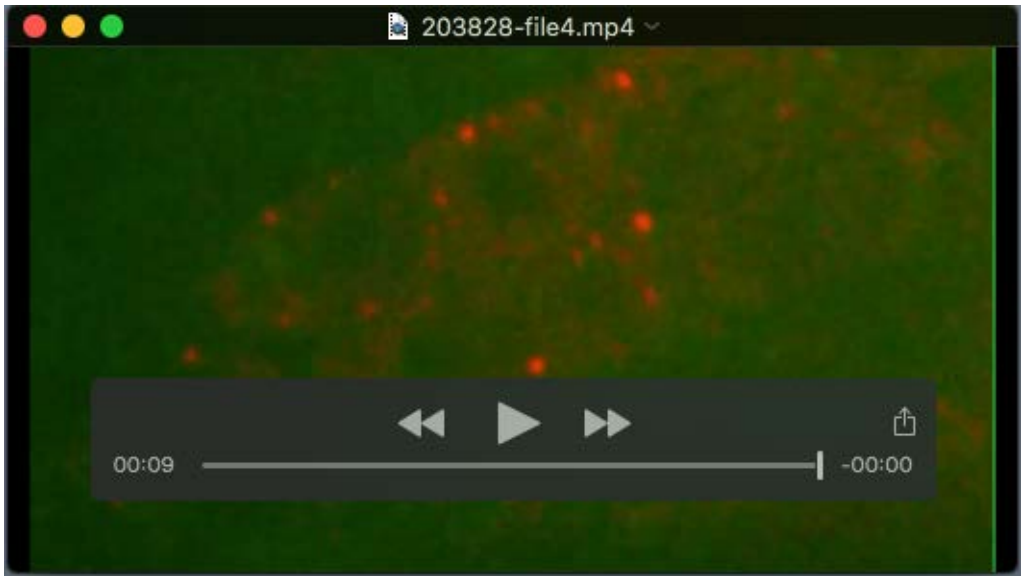

Movie 3. Spinning-disc confocal microscopy of AGD1-GFP foci and ARA6-mCherry (LE/PVC marker) in root cap cells. Total elapsed time is about 1 minute.

Journal of Cell Science • Supplementary information